NPS ARCHIVE
1968
BRUNO, M.

EXPERIMENTAL TECHNIQUES TO DETERMINE Ntu OF COMPACT HEAT EXCHANGER SURFACES

by

Marco Joseph Bruno

DUDLEY KNOX LIBRARY
NAVAL POSTGRADUATE SCHOOL
MONTEREY CA 93943-5101

Gaylord
SHELF BINDER
Syracuse, N. Y.
Stockton, Calif.

UNITED STATES
NAVAL POSTGRADUATE SCHOOL

THESIS

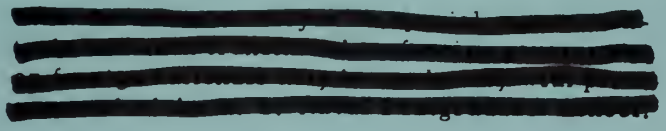
EXPERIMENTAL TECHNIQUES TO DETERMINE

N_{tu} OF COMPACT HEAT EXCHANGER SURFACES

by

Marco Joseph Bruno

September 1968



[redacted]

EXPERIMENTAL TECHNIQUES TO DETERMINE N_{tu} OF COMPACT HEAT EXCHANGER SURFACES

by

Marco Joseph Bruno
Lieutenant, United States Navy
B.S., Naval Academy, 1961

Submitted in partial fulfillment of the
requirements for the degree of

MASTER OF SCIENCE IN MECHANICAL ENGINEERING

from the

NAVAL POSTGRADUATE SCHOOL
September 1968

1968
BRUNO, M.

ABSTRACT

Two new transient testing techniques were evaluated; the centroid method developed by Kohlmayr and the time zero intercept technique. The zero intercept method was found to be the most promising of the two but is limited to values of $N_{tu} < 2.5$. The centroid technique can be used effectively when the value of N_{tu} is less than 5.0.

A heater system made of .001 inch diameter nichrome wire was designed and tested to determine its effect on the transient testing of matrix type heat exchangers. Because the design showed no improvement in the test results and was unreliable its use was discontinued.

LIBRARY
NAVAL POSTGRADUATE SCHOOL
MONTEREY, CALIF. 93940

TABLE OF CONTENTS

Section		Page
1.	Introduction	13
2.	Summary of Theory	15
3.	Experimental Techniques	25
4.	Description of Test Matrices	28
5.	Presentation of Results	29
6.	Discussion of Results	30
7.	Experimental Uncertainties	33
8.	Conclusions	39
9.	Recommendations for Further Study	41
10.	Bibliography	42

Appendix A	Description of Equipment	44
Appendix B	Data Reduction Relationships	47
Appendix C	Determination of Facility Transient Response	54

LIST OF TABLES

Table		Page
I.	Summary of Heat Transfer and Flow Friction Results for Core T20-38	75
II.	Summary of Heat Transfer and Flow Friction Results for Core Solar 4	76
III.	N_{tu} as a Function of Maximum Slope and Longitudinal Conduction Parameter	77

LIST OF FIGURES

Figure		Page
1.	μ_{CENTD} versus N_{tu}	57
2.	Sample Recording of Temperature Responses	58
3.	Experimental Set-up	59
4.	Matrix Holder and Test Section	60
5.	Schematic of Test Apparatus	61
6.	Geometric and Physical Properties of Core T20-38	62
7.	Geometric and Physical Properties of Core Solar 4	63
8.	Core T20-38 Test Results	64
9.	Core Solar 4 Test Results	65
10.	Core Solar 4 Test Results	66
11.	Comparison of Maximum Slope Test Results of Core Solar 4, with .003 in. and .001 in. Heaters	67
12.	Heater Time Constant, θ_H versus Flow Rate	68
13.	Error in Maximum Slope Due to Deviation From Step	69
14.	N_{tu} versus Maximum Slope with Conduction Parameter (Max. slope, .3-2.05)	70
15.	N_{tu} versus Maximum Slope with Conduction Parameter (Max. slope, .3-1.7)	71
16.	Finding μ_{CENTD} from Temperature-Time Trace	72
17.	Finding t_f^* from Normalized Temperature-Time Trace	73
18.	Photo of .003 in. Wire and .001 in. Wire Heater Frames	74

NOMENCLATURE

English Letter Symbols

A	Matrix total heat transfer area	sq ft
A_c	Matrix minimum free flow area	sq ft
A_{fr}	Matrix total frontal area	sq ft
A_s	Matrix solid cross-sectional area available for thermal conduction	sq ft
a_s	Fin thickness	ft
b	Flow passage perimeter (βA_{fr})	ft
C_f	Fluid stream thermal capacity rate ($\dot{m}c_f$)	Btu/(hr deg F)
c_f	Fluid specific heat	Btu/(lbm deg F)
C_s	Matrix thermal capacity ($W_s c_s$)	Btu/deg F
c_p	Fluid specific heat at constant pressure	Btu/(lbm deg F)
c_s	Matrix material specific heat	Btu/(lbm deg F)
D_H	Flow passage hydraulic diameter ($4r_h$)	ft
E	Friction power per unit area	hp/sq ft
G	Flow stream mass velocity ($\dot{m}/A_c$)	lbm/(hr sq ft)
g_c	Proportionality factor in Newton's Second Law	32.2 (lbm ft)/(lbf sec^2)
g	Normalized fluid temperature at inlet to test section	dimensionless
h	Surface heat transfer coefficient for convection; heat transfer power per unit area per degree temperature difference	Btu/(hr sq ft deg F)
$I(g)$	Deviation from step	dimensionless
k	Fluid thermal conductivity	Btu/(hr sq ft deg F/ft)
k_s	Matrix thermal conductivity	Btu/(hr sq ft deg F/ft)

L	Total matrix flow length	ft
$\dot{m}$	Mass flow rate	lbm/hr
P	Pressure	lbf/sq ft
p	Matrix porosity (A_c/A_{fr})	dimensionless
q	Heat transfer rate	Btu/hr
R	Gas constant (53.35-air)	(ft lbf)/(lbm deg R)
r_h	Hydraulic radius ($A_c L/A$)	ft
t	Temperature	deg F
t*	Normalized temperature	dimensionless
u	Flow velocity	ft/sec
V_m	Matrix volume	cu ft
W_s	Matrix mass	lbm
W_f	Fluid mass in matrix	lbm
x	Distance along flow passage from the matrix inlet	ft
Z	Reduced length ($N_{tu} \frac{x}{L}$)	dimensionless

Greek Letter Symbols

β	Compactness (A/V_m)	sq ft/cu ft
$\bar{\beta}$	Ratio of orifice diameter to pipe diameter (d_o/d)	dimensionless
Δ	Difference or change (time, temperature, distance, etc.)	
θ	Time	sec, hr
μ	Free time	dimensionless
$\bar{\mu}$	Fluid viscosity	lbm/hr ft
μ_{CENTD}	Centroid coordinate	dimensionless
ρ	Density	lbm/cu ft

Subscripts

atm	Local atmosphere
ave	Average
f	Fluid (gas, air)
i	Initial, inlet
m	Matrix, mean
o	At orifice
s	Solid (Matrix material), static
STD	Standard (temperature and pressure)
x	Local conditions
1	Inlet conditions (upstream of matrix and heaters)
2	Inlet conditions at matrix entrance
3	Exit conditions at matrix outlet

Dimensionless Groupings

f	Fanning friction factor; ratio of wall shear stress to fluid dynamic head
j	Colburn j-factor ($N_{St} N_{Pr}^{2/3}$). This factor plotted vs. Reynolds Number defines the surface heat transfer characteristics.
λ	Longitudinal heat conduction parameter for solid material ($k_s A_s / \dot{m} L c_f$)
γ	Time parameter ($hA\theta / W_s c_s$)

ACKNOWLEDGEMENT

The author would like to thank Dr. Paul F. Pucci, Professor of Mechanical Engineering, for his help during this work.

1. Introduction.

The transient test facility at the Naval Postgraduate School(NPS) has been in operation for several years. Two techniques have been used at the NPS facility for the determination of heat transfer data. One of these is the maximum slope technique developed by Locke [13] which utilizes the temperature-time response curve of the fluid leaving the matrix after a step change in the fluid inlet temperature. Howard [6] extended this technique to include the effects of longitudinal conduction. The other technique is the cyclic technique developed by Bell and Katz [4]. In both of these techniques the heat transfer parameter being sought is N_{tu}, which is a dimensionless heat transfer parameter equal to the ratio of the convective heat transfer rate from a solid to the heating capacity rate of an adjacent fluid, i.e.,

$$N_{tu} = \frac{hA}{\dot{m} c_f}$$

where:

h = unit conductance for convection heat transfer (BTU/hr sq ft deg F)

A = total heat transfer area of solid (sq ft)

$\dot{m}$ = mass flow rate of fluid (lbm/hr)

c_f = specific heat of fluid (Btu/lbm deg F)

It is known that the maximum slope technique is unreliable at values of N_{tu} less than 3.5, due to the large errors in N_{tu} associated with errors in the determination of maximum slope. Furthermore, it has been noted experimentally that for values of N_{tu} near 2.0, the temperature response curve of a fluid displayed its maximum slope at approximately time zero on the trace, and that this value of maximum slope was not suited for determining N_{tu}.

It was not until the work done by Kohlmayr [9, 10], which gave the exact analytical solution to the single-blow problem based on Hausen's [5] mathematical model, that the reason for these errors was fully understood. Later work by Kohlmayr [11, 12] demonstrated ways in which to handle this problem as well as the development of a new technique which might be used in place of the maximum slope technique for values of $N_{tu} < 5$. Kohlmayr also developed a means to handle the single-blow problem when other than a step change in the inlet fluid temperature was made.

The purpose of this thesis was first to determine experimentally the actual inlet temperature response of the NPS facility and to use this known temperature response in the manner suggested by Kohlmayr. Additionally, a new heater system was made to try to more closely approximate a step change in the fluid inlet temperature so that the physical process and mathematical model might more closely resemble one another, thereby improving the results using the maximum slope technique.

Another technique, the "time zero intercept technique," used by Wheeler [17] was investigated.

2. Summary of Theory.

A. Background

The single-blow transient technique which is used to determine heat transfer data for a porous solid originally used for its mathematical model Hausen's [5] partial differential equation system. The method involved comparing the recorded exit temperature of a fluid passing through a porous solid which had previously undergone a step change in its temperature, with a computed response curve based on the solution to Hausen's equations.

Locke [13] has shown that there exists a unique relationship between the maximum slope of the response curves and the number of heat transfer units, N_{tu}. However, Hausen's model did not include the effects of longitudinal conduction. Howard [6], by the use of a finite difference technique with the digital computer, included the effects of longitudinal conduction.

It should be noted here that in all of Kohlmayr's work, which will be discussed later, the effects of longitudinal conduction are not considered.

B. Theory

The basic assumptions in the single-blow problem are:

(1) Properties of the fluid are temperature independent

(2) Fluid flow is steady

(3) The porous solid is homogeneous

(4) The thermal conductivity of both solid and fluid is infinite in the direction perpendicular to flow

(5) Thermal conductivity of the solid is zero in the direction of flow

Hausen's original differential equation system [5] was based on the energy balance between a fluid passing through a porous solid and the solid. The system of differential equations which resulted from this development are as follows:

$$\frac{\partial t_f}{\partial z} + t_f = t_s$$

$$\frac{\partial t_s}{\partial \tau} + t_s = t_f$$

in which a "reduced length" variable,

$$z = \frac{hAx}{\dot{m} c_f L} = N_{tu} \frac{x}{L}$$

and a dimensionless time parameter,

$$\tau = \frac{hA}{W_s c_s} \theta - \frac{hAx}{\dot{m} L c_f} \left(\frac{W_f c_f}{W_s c_s} \right)$$

have been used.

In the above equations:

t_s = temperature of the solid (deg F)

t_f = temperature of the fluid (deg F)

θ = time (hr)

c_s = specific heat of the solid (Btu/lbm deg F)

W_s = mass of the solid (lbm)

x = distance along flow passage measured from inlet (ft)

L = total length of solid (ft)

W_f = mass of fluid entrained in solid (lbm)

Kohlmayr [11] has modified Hausen's original equations by introducing a new dimensionless time variable called "free time,"

$$\mu = \frac{\dot{m} c_f}{W_s c_s} \theta - \frac{W_f c_f}{W_s c_s} \frac{x}{L} \qquad (1)$$

or

$$\mu = \frac{\tau}{N_{tu}} \tag{2}$$

For convenience Kohlmayr introduced two constants,

$$\alpha = \frac{\dot{m} c_f}{W_s c_s} \qquad \text{and} \qquad \beta = \frac{W_f c_f}{W_s c_s}$$

which are fixed for any particular experiment. For most practical purposes, $\beta \approx 0$ and $\mu \approx \alpha\theta$.

Hausen's modified equations are then given as

$$\frac{\partial t_f^*(z,\mu)}{\partial z} + t_f^*(z,\mu) = t_s^*(z,\mu) \tag{3}$$

$$\frac{\partial t_s^*(z,\mu)}{N_{tu}\,\partial \mu} + t_s^*(z,\mu) = t_f^*(z,\mu) \tag{4}$$

where t_s^* and t_f^* are the temperatures of the solid and fluid respectively, which have arbitrarily been normalized. The above equations are subject to the boundary and initial conditions:

at $z = 0$ $\qquad t_f^*(z,\mu) = g(\mu)$ (5)

and

at $\mu = 0$ $\qquad t_s^*(z,\mu) = 1$ (6)

where $g(\mu)$ represents the normalized, time-dependent fluid temperature at the inlet cross-section. Kohlmayr solved equations (3) through (6) by means of a double Laplace Transform [10].

The results of Kohlmayr's solution are:

$$t_f^*(z,\mu) = e^{-z}\left[g(\mu) + \int_0^{\mu} z N_{tu} \Xi_1\left(z N_{tu}(\mu-\nu)\right) e^{-N_{tu}(\mu-\nu)} g(\nu)\, d\nu\right]$$

$$+ 1 - e^{-z}\left[1 + \int_0^{\mu} z N_{tu} \Xi_1\left(z N_{tu}\nu\right) e^{-N_{tu}\nu}\, d\nu\right] \tag{7}$$

Ξ_K is an entire family of functions of the order $K (K=0,1,..,n)$

i.e.,

$$\Xi_K(X) = \sum_{n=0}^{\infty} \frac{X}{n!(n+K)!}$$

Evaluated at

$$Z\big|_{x=L} = N_{tu} \tag{8}$$

equation (7) becomes

$$t_f^*(N_{tu},\mu) = 1 - e^{-N_{tu}} \left[1 - g(\mu) + \int_0^{\mu} N_{tu}^2 \Xi_1(N_{tu}^2(\nu-\mu)) e^{-N_{tu}(\nu-\mu)} (1-g(\nu)) d\nu \right] \tag{9}$$

By differentiation of equation (9) with respect to μ ,

$$\frac{\partial t_f^*(N_{tu},\mu)}{\partial \mu} = e^{-N_{tu}} \left\{ \frac{\partial g(\mu)}{\partial \mu} + N_{tu}^2 g(\mu) - N_{tu}^2 e^{-N_{tu}\mu} \Xi_1(N_{tu}^2 \mu) \right.$$

$$\left. + \int_0^{\mu} N_{tu}^3 \left[N_{tu} \Xi_2(N_{tu}^2(\mu-\nu)) - \Xi_1(N_{tu}^2(\mu-\nu)) \right] e^{-N_{tu}(\mu-\nu)} g(\nu) d\nu \right\} \tag{10}$$

With these results Kohlmayr [12] then showed that for other than a step change in inlet temperature, both the maximum slope and "free time" at a given value of N_{tu} may be multi-valued. He further demonstrated that by knowing what the inlet response is, one can determine which of the values of maximum slope is valid and also how to determine what the error bounds are in the use of some known inlet temperature change. One of Kohlmayr's results is that the correct value of "relative" maximum slope occurring in the fluid exit temperature response will be that value

which occurred last in cases in which Kohlmayr's technique is applicable. Furthermore, the maximum slope method is unstable for $N_{tu} < 2.0$, is singular at $N_{tu} = 2.0$, and inaccurate for N_{tu} between 2.0 and 3.0. [9,12]

In view of the short-comings of the maximum slope technique, Kohlmayr developed an indirect curve-matching technique [11]. Some important results of this development are summarized below.

With the solution to the single-blow problem known, it is possible to develop an indirect curve-matching technique based on the first moments of the fluid transient response curves. This method, known as the centroid method, involves the reducing of both the theoretical temperature response $t^*_f(N_{tu}, \mu)$ and experimental response $t^*_{fexp}(N_{tu}, \mu)$ into two different single-valued functions based on the one parameter N_{tu}. To generalize the problem further, a mapping functional was defined, based on the fluid inlet temperature change and the fluid's exit temperature response such that

$$\chi(N_{tu}) = \chi\left(t^*_f(N_{tu}, \mu), g(\mu)\right)$$

where the following restrictions are imposed on χ:

(1) χ must be real, single-valued, continuous with respect to both $t^*_f(N_{tu}, \mu)$ and $g(\mu)$, and monotone with the parameter N_{tu}.

(2) $\chi(N_{tu})$ must be monotone increasing with $I(g) = \int_0^\infty g(\mu)\,d\mu$, the "deviation from step."

(3) $\left|\frac{d\chi(N_{tu})}{dN_{tu}}\right| \geq K$, where K is some measure for the maximum permissible amplification of errors.

(4) For any N_{tu} and any given deviation from step, $\chi(N_{tu})$ should be insensitive with respect to local variations of $g(\mu)$.

(5) The evaluation of $\mathcal{Y}(N_{tu})$ must be simple and straightforward.

The functional chosen was the first moment of the difference between upstream and downstream fluid temperatures,

$$\int_0^\infty \mu \left[t_f^*(N_{tu}, \mu) - g(\mu) \right] d\mu = \frac{1}{2} + \frac{1}{N_{tu}} + \int_0^\infty g(\mu)\, d\mu \qquad (11)$$

Due to the difficulty involved with integrating equation (11) up to values of $\mu = \infty$, a new functional was chosen and defined as

$$\int_0^{\mu_{1/10}} \mu \left[t_f^*(N_{tu}, \mu) - g(\mu) \right] d\mu = \frac{1}{2} + \frac{1}{N_{tu}} + \int_0^\infty g(\mu)\, d\mu \qquad (12)$$

Some further restrictions imposed upon $g(\mu)$ are:

(1) $g(\mu)$ must be non-negative monotone decreasing

(2) have initial value $g(0) = 1$ and

(3) assume value zero for all free times which exceed the maximum permissible deviation from step: $g(\mu) = 0$ for all $\mu \geq I_{max}$.

Therefore the moment functional was defined in terms of the centroid of the area under this difference curve:

$$\mu_{CENTD} = \frac{\int_0^{\mu_{1/10}} \mu \left[t_f^*(N_{tu}, \mu) - g(\mu) \right] d\mu}{\int_0^{\mu_{1/10}} \left[t_f^*(N_{tu}, \mu) - g(\mu) \right] d\mu} \qquad (13)$$

For the case of $g(\mu) = 0$ (step change), the results of equation (13) are listed as Figure 1.

In order to use the above results for any given inlet temperature change $g(\mu)$, Kohlmayr arrived at the following empirical relationship:

$$\mu_{CENTD}(N_{tu}, g) \cong \mu_{CENTD}(N_{tu}, 0) + .99\, I(g) \pm .01 \qquad (14)$$

This relationship was obtained by systematically applying the centroid method to many different upstream fluid temperature changes.

Kohlmayr's solution to the single-blow problem may also be used directly. Returning again to equations (9) and (1)

$$t_f^*(N_{tu}, \mu) = 1 - e^{-N_{tu}} \left[1 - g(\mu) + \int_0^{\mu} N_{tu}^2 \, \Xi_1(N_{tu}^2(\nu - \mu)) \, e^{-N_{tu}(\nu - \mu)} (1 - g(\nu)) \, d\nu \right]$$

where

$$\mu = \frac{m c_f \Theta}{W_s c_s} - \frac{W_f c_f}{W_s c_s} \frac{x}{L}$$

$t_f^*(N_{tu}, \mu)$ can be evaluated at "free time," $\mu = 0$, which would correspond to the time that an element of fluid which has undergone a change in temperature upstream arrives at the exit of the solid. Thus,

$$t_f^*(N_{tu}, 0) = 1 - e^{-N_{tu}} \left[1 - g(0) \right] \qquad (15)$$

or

$$1 - t_f^*(N_{tu}, 0) = e^{-N_{tu}} \left[1 - g(0) \right] \tag{16}$$

Taking the natural logarithm of both sides of the above equation, yields

$$\ln \left[1 - t_f^*(N_{tu}, 0) \right] = - N_{tu} + \ln \left[1 - g(0) \right] \tag{17}$$

Therefore

$$N_{tu} = - \ln \left[1 - t_f^*(N_{tu}, 0) \right] + \ln \left[1 - g(0) \right] \tag{18}$$

Note that for a step change in the inlet temperature, i.e., $g(\mu) = 0$ for $\mu > 0$, that equation (18) reduces to,

$$N_{tu} = - \ln \left[1 - t_f^*(N_{tu}, 0) \right] \tag{19}$$

In order to utilize equation (19) directly it would be necessary to achieve a step change in the inlet fluid temperature, $g(\mu)$. This would occur at real time, $\theta = 0$. Then measure the temperature of that same element of fluid which had undergone the step change in temperature, as it left the porous solid. This would occur at "free time," $\mu = 0$.

Because of the finite response time of the different components of the experimental equipment, i.e., heaters, thermocouples and recorder, it is not possible to meet precisely either of the above requirements. In view of the above limitations it is necessary either to make some approximations in the interpretation of the temperature response data, t_f^*, or else devise a means by which the actual response data might be treated directly. Some of the difficulties involved with the second alternative are: Refer again to equation (9)

$$t_f^*(N_{tu},\mu) = 1 - e^{-N_{tu}} \left[1 - g(\mu) + \int_0^{\mu} N_{tu}^2 \Xi_1(N_{tu}^2(\nu-\mu))\, e^{-N_{tu}(\nu-\mu)} (1-g(\mu))\, d\nu \right]$$

which may be stated as

$$N_{tu} = -\ln\left[1 - t_f^*(N_{tu},\mu)\right] + \ln\left[1 - g(\mu) + \int_0^{\mu} N_{tu}^2 \Xi_1(N_{tu}^2(\nu-\mu))\, e^{-N_{tu}(\nu-\mu)} (1-g(\mu))\, d\nu \right]$$

and the expression for the inlet fluid temperature,

$$g(\mu) = e^{-\frac{1}{\alpha\theta_H}(\mu+\beta)},$$

where θ_H is the equal to the heater time constant which was derived in Appendix C.

One approach to using equation (9) would be to measure t_f^* at some value of "free time" $\mu > 0$ such that $g(\mu) \cong 0$ for which N_{tu} would be,

$$N_{tu} = -\ln(1 - t_f^*) + \ln\left[1 + \int_0^{\mu} N_{tu}^2 \Xi_1(N_{tu}^2(\nu-\mu))\, e^{-N_{tu}(\nu-\mu)} (1-g(\nu))\, d\nu \right]$$

The difficulty here is, that in order to evaluate

$$\int_0^{\mu} N_{tu}^2 \Xi_1(N_{tu}^2(\nu-\mu))\, e^{-N_{tu}(\nu-\mu)} (1-g(\nu))\, d\nu$$

N_{tu} must first be known. This would result in a direct curve matching technique. A second approach would be to measure t_f^* at some time $\mu > 0$ such that

$$g(\mu) = \int_0^{\mu} N_{tu}^2 \Xi_1(N_{tu}^2(\nu-\mu)) e^{-N_{tu}(\nu-\mu)} (1-g(\mu)) d\mu$$

again N_{tu} must first be known. In both the above methods if μ is small the transient response of the sensing and recording equipment will still present problems.

Because of the difficulties encountered with the above two methods, the first alternative, that of making some approximations in the interpretation of the measured response data, t_f^*, will be considered. Since the response of the thermocouples is faster than that of the .003" diameter heaters, and approximately equal to that of the .001" heaters, see Appendix C, it might be reasonable to assume that the initial response recorded during a particular run is that response due to the heaters, see Figure 2B. Therefore, it is possible to extrapolate back to "free time" $\mu = 0$, from the time on the response curve where the transient response of the heaters has died out and treat the intersection of the extrapolated curve and "free time," $\mu = 0$ as an actual step change in temperature. The above technique is referred to as the "zero intercept" technique.

3. Experimental Technique.

The existing apparatus at the NPS facility, see Figures 3 and 4, has been designed to conform to the idealizations required by Howard [5] for the use of his conduction parameter in the maximum slope technique. Howard's conduction parameter, λ, is defined as

$$\lambda = \frac{k_s A_s}{\dot{m} L c_f}$$

where:

k_s = thermal conductivity of the solid (Btu/hr sq ft deg F/ft)

A_s = matrix solid cross-sectional area available for thermal conduction (sq ft)

Howard's idealizations are as follows:

(1) The fluid flow in the matrix is both steady and uniform in velocity and temperature at any cross section

(2) The matrix thermal conductivity is finite in the direction parallel to fluid flow and infinite in the direction normal to flow

(3) The matrix thermal conductivity is large in comparison to that of the contained fluid

(4) The thermal properties of the fluid and matrix are constant and uniform

(5) The convective heat transfer coefficient is some suitable average and remains constant

(6) A step change in the temperature of the inlet fluid is imposed at real time equal to zero.

These idealizations result in making the fluid flow one dimensional. They in no way conflict with the restrictions imposed by Kohlmayr [11].

The requirement of uniform velocity and temperature profiles (1) is met by a specially designed entrance nozzle, flow straightening screens, and an even distribution of heater wires across the channel.

Piersall [15], using the equipment, verified that the velocity and temperature profiles were, indeed, uniform within reasonable limits. The importance of uniform velocity and temperature profiles was demonstrated by Wheeler [17].

The small temperature change across the matrix of about 20°F gives constant thermal properties of the fluid and matrix and a constant heat transfer coefficient as required by idealizations (5) and (6).

The restriction that the temperature of the inlet fluid be subjected to a step change will be discussed later.

The data required for the computation of the various heat transfer, fluid flow coefficients, and dimensionless parameters is as follows:

P_{ATM} = atmospheric pressure (mm Hg)

P_o = orifice static pressure (inches H_2O)

ΔP_o = pressure drop across orifice (inches H_2O)

ΔP_M = pressure drop across matrix (inches H_2O)

P_s = static inlet pressure at entrance to heaters (inches H_2O)

t_o = temperature of fluid at orifice (millivolts)

d_o = orifice diameter

$\bar{\beta}$ = ratio of orifice diameter to pipe diameter

CS = chart speed (sec/inch)

t_3-t_1 = downstream response

t_3-t_2 = downstream - upstream response

Pressures are measured with either a draft gage or a water manometer, depending upon the orifice-flow rate combination, except for atmospheric pressure which is measured by a mercury barometer.

The temperature responses recorded are t_3-t_1, the difference between the inlet fluid temperature and the fluid temperature at the matrix exit

(used in the maximum slope and zero intercept techniques) and t_3-t_2, the difference between the fluid exit temperature and the matrix inlet fluid temperature (used in the centroid technique). For a more complete description of equipment, the reader is referred to Appendix A. See Figure 5 for the position of temperature and pressure measurements.

A test run is accomplished by predetermining the necessary pressure drop across the orifice to achieve a desired flow rate and to determine the number of heaters necessary to achieve a 20°F temperature rise. Air is drawn through the apparatus and is controlled at the entrance to the turbocompressor. When the desired flow rate is achieved the heaters are then energized and the heated air and test core are allowed to reach a steady state temperature, at which time pressure measurements are recorded. Power to the heaters is then secured and recordings of t_3-t_1 and t_3-t_2, both as functions of time are recorded on separate channels of the Brush recorder (see Figures 2A and B). The temperature at the orifice (t_0) is measured before and after a run to insure the same ambient air temperature for the run.

After completion of the desired runs, the values needed to compute slope are taken from the recorded traces of t_3-t_1. The maximum value of slope is obtained visually with the aid of a straight edge. This information is included on the data sheet. The data sheet layout conforms to the data input section of a digital computer program [18], which reduces the data used in the maximum slope technique and calculates the parameter α used in the centroid technique. For complete details on data reduction the reader is referred to Appendix B at this time.

4. Description of Test Matrices.

The two cores used in this experiment were both cores which had been tested previously and for which there was a good deal of data available.

One matrix, the Cercor T20-38, previously tested by Howard [7], is a ceramic type-core having a low thermal conductivity, and was used to eliminate any errors that might be introduced by longitudinal conduction which might have invalidated results using the centroid and zero intercept techniques. The other core tested, which is a stainless steel plate-fin type matrix, Solar 4, had been tested several times [15], [16], [18] and was used so that comparisons could be made when longitudinal conduction was a factor.

Further information on core geometries and properties is shown in Figures 6 and 7.

5. Presentation of Results.

For each matrix tested, the heat transfer and flow friction characteristics have been computed. The computed results are shown tabulated in Tables I-II. The values of N_{tu} have been plotted for the three methods used in this experiment. Figures 8A and 9 compare values of N_{tu} based on the maximum slope and centroidal technique for cores T20-38 and Solar 4. Figures 8B and 10 compare values of N_{tu} based on the maximum slope and zero intercept technique for the same two cores. Figure 11 is a comparison of N_{tu} values computed by the maximum slope technique for the two heater systems. Core Solar 4 was the only core tested with the new .001 inch diameter wire heaters.

The heater response curves are shown in Figure 12. See Appendix C for complete details used in determining these curves.

6. Discussion of Results

In order to insure that the technique used by the author in this experiment was correct, the results of the single-blow test of this experiment were compared with the results of previous tests of the same cores.

Considerable difficulty was experienced in the use of the new (.001 inch diameter) heater system. The heaters burned out frequently, thereby limiting the range of Reynolds Numbers over which the core was tested and also the number of cores actually tested. The exact reason for the burnout is not known. It was initially thought to be due to surges in current caused by the use of a resistor bank in the first experiments. However, when the resistor bank was removed and voltage to the heaters controlled by the motor generator set rheostat, the system failed again. In all, there were three different failures, all occurring at different flow rates and with a different number of heaters in use at the time of failure.

An examination of Figure 11 shows that in the high Reynolds number ranges there is little difference in the value of N_{tu} based on the maximum slope data for the two different heater systems. Furthermore, this is in a range where the errors in N_{tu} due to errors in the maximum slope technique are greatest. Without actually applying Kohlmayr's equations in the "extension of the maximum slope" technique [17], it is impossible to get a quantitative value for the error in N_{tu} due to deviations from the step change. However, by the use of his curves based on the "deviation from step" (previously defined as I(g) and equal to the area under the inlet-temperature response curve) which are presented here as Figure 13, it can be seen that for $I < .100$ the error in slope, Δm which is the difference in the maximum slope due to a step change in the inlet fluid minus the maximum slope due to a non-step change in the inlet fluid, is less than

.01. It must be pointed out that Figure 13, is for an upstream temperature change which is quadratic, i.e., $g(\mu) = (1-\mu/A)^2$. The curves of Δm versus N_{tu} for the NPS facility would be slightly different from those presented in Figure 13, for the $g(\mu)$'s associated with the NPS facility's heater systems are exponential. However, for low values of $I(I < .100)$ the error in maximum slope Δm would be small regardless of the exact form of the inlet temperature response. Since the maximum I(g) resulting from either heater system is less than .03 it would not be expected for one to detect any difference of slope and consequently N_{tu} resulting from the use of either system.

Again referring to Kohlmayr's curves, Figure 13, deviations from step changes in temperatures would cause large errors at lower flow rates, i.e., $N_{tu} > 5$. However, since the I(g) of the NPS facility decreases with decreasing flow rates (see Appendix C) it could be assumed that the errors in maximum slope due to I(g) would be small. Furthermore, since the longitudinal conduction is greater at low flow rates its' effects cannot be neglected as they have in Kohlmayr's assumptions.

In the investigation of the centroid and the zero intercept techniques the range of flow rates of both cores tested was the same and ranged from $\dot{m} \approx$ 250 to $\dot{m} \approx$ 950 lbm/hr. The reason for 950 lbm/hr being the maximum value tested was that at this flow rate all heaters were in use and in order to go to higher flow rates, an increase in voltage would have been necessary to achieve the same 20 deg F. temperature rise. This would have changed the heater time constant, which is a function of both flow rate and the number of heaters in use.

Investigation of the curves of Figure 8A and 9 reveals that for both cores tested there is very close agreement between the results predicted by the maximum slope technique, shown as the dotted line, and the results

of the centroid technique for values of N_{tu} between 3.5 and 5. In fact there is even some overlapping of points in Figure 8A. For values of N_{tu} below 3.5, the values of N_{tu} based on the maximum slope technique begin to decrease from the predicted values whereas the values determined using the centroid technique followed closely the predicted values for the case of Solar 4 and increased slightly from the predicted values for core T20-38.

It can be seen from Figure 8B, which compares the values of N_{tu} computed by the maximum slope and zero intercept method, for core T20-38, that the flow rates used were not high enough for the zero intercept method to be used to its best advantage. Only those runs made at flow rates greater than 600 lbm/hr had a clearly measurable zero intercept.

Figure 10 again compared maximum slope N_{tu}'s with those evaluated by the zero intercept technique in this case for core Solar 4. This was done for both sets of heaters. It is important to note the close correlation between the values of N_{tu} for the two heater systems. This will be covered more fully in Section 7.

7. Experimental Uncertainties.

Various idealizations and boundary conditions have been imposed for the mathematical model of the physical experiment. Due to the fact that these idealizations and boundary conditions have not been precisely met, certain errors have been introduced. These errors are difficult to assign a numerical value to, and with the exception of the deviation from step temperature change previously mentioned and the effects of longitudinal conduction, will not be discussed.

The experimental errors associated with the maximum slope technique used at the NPS facility have been covered in considerable detail, [2][3] [15]; therefore only those errors introduced in this particular experiment will be discussed.

In using Kohlmayr's centroidal technique there are several sources of possible error. First, Kohlmayr, in using Hausen's mathematical model has neglected longitudinal conduction in the solid. Howard [6] has calculated the errors in N_{tu} associated with longitudinal conduction in using the maximum slope technique, but no such information is available for use with the centroidal technique, for the analytical solution to the single-blow problem, in this case, does not include the effects of longitudinal conduction. Therefore, one can only get a qualitative idea as to the effects of these errors.

From Howard's curves of N_{tu} versus maximum slope, Figures 14 and 15, for a given value of N_{tu} the slope of a temperature response curve is different for different values of the conduction parameter λ . Therefore, the response curves and consequently the centroid of the response curves would be different for different values of λ . The difference in maximum slope due to λ decreases as N_{tu} decreases. For example at N_{tu}= 30 a difference in λ of approximately .1 causes a 90% difference in

maximum slope, whereas for $N_{tu} < 5$ the maximum error in maximum slope caused by a .1 difference in λ is approximately 9%. It would seem reasonable to assume that provided Kohlmayr's results were applied only in the low N_{tu} range ($N_{tu} < 5$) and longitudinal conduction was small (i.e., $\lambda < .1$), conduction errors could be neglected. For this experiment the maximum value of λ for either core at values of $N_{tu} < 5$ was less than .022.

Another source of error is in the determination of the centroid of the area under the response curve. Two methods were used for this experiment, primarily as checks on each other. In both methods the critical point is the determination of where the cut-off is for a particular curve. The cut-off point is that point on the response curve which is one-tenth of the maximum value. This point, defined as $\mu_{1/10}$ occurs at a point where the slope of the curve is slowly approaching zero, and an error of one millimeter in the ordinate can cause an error of several millimeters in the abscissa. For example, in the data taken with core Solar 4 when $N_{tu} = 1.41$, at $(t_3-t_2) = 6$mm, $\Theta = 13.0$ sec., and for $(t_3-t_2) = 5$, $\Theta = 13.75$ sec. This was for a typical trace in which $(t_3-t_2)_{max} = 50.5$mm. A sketch of the response curve (see Figure 16) will help to clarify the problem.

The actual error in μ_{CENTD} caused by an error in determining $\mu_{1/10}$ will depend on the value of N_{tu}. A typical example would be for $N_{tu} = 3.5$. When computed by the manual technique (see Appendix B for details), it was found that a $\pm$ 1 mm difference in ordinate (which is $\approx$ 2% and would be a maximum) caused an error of $\approx$ 2% in μ_{CENTD}. It should be pointed out that these values are approximate, for there is some uncertainty associated with finding the intersection of the three centers of mass

lines, shown in Figure 16 and discussed in Appendix B. This uncertainty usually was less than ± 2%. The same type of error associated with finding the cutoff point is also found in the computer technique of determining the centroid. In this method the computer solution required data points from the response curve at fixed intervals, which for this experiment were 5mm intervals. Therefore, if the value of $\mu_{1/10}$ occurred at a point midway in any one 5mm increment, there could be as much as a 2½ mm error in the cut-off. For an average 130 to 140 mm trace this is less than 2%. For comparative purposes, data runs were made using both techniques and the maximum deviation in centroid between the two methods was found to be 4%, but the majority of deviations was less than 1%.

Another difficulty discovered in analyzing the temperature trace was caused by the sensitivity of the thermocouples. During a particular run a change in the steady flow caused by a sudden draft in the laboratory caused a temperature deviation on the trace. This required some visual smoothing on the part of the author to extrapolate the actual response. This might cause errors when using an automated data reduction process, unless it included a good smoothing technique.

An additional problem was encountered in the process of data reduction. One of the assumptions made in using the centroid technique is that at time zero the temperature both upstream and downstream from the matrix is constant. It was found that this was not the case for this experiment, the reason being that there was some heating of the thermocouples located adjacent to the heaters due to radiation from the heaters. This meant that the zero reference point of the trace of (t_3-t_2) established before and after the run (heaters off) was not the same as that just prior to time zero when the heaters were deenergized (see Fig. 16). Therefore,

where the response curve should have resembled curve a of Fig. 16, it took the form of curve b. To compensate for this, point c was taken as time zero and curve a used to determine the centroid. It should be pointed out here that these figures are greatly exaggerated here for clarity and the error caused by this difference is felt to be negligible. Also, this difference was most evident at low flow rates, for the radiation effect was caused primarily by the heaters nearest the thermocouples. As the flow rates increased and more heaters were energized the percentage of heating due to radiation became less.

So far no mention has been made of the error in N_{tu} caused by an error in μ_{CENTD}. Kohlmayr [11] has conducted a linear error analysis based on the approximation

$$\Delta N_{tu} \cong \frac{d N_{tu}}{d \mu_{CENTD}} \Delta \mu_{CENTD}$$

and introduced a relative error amplification factor

$$K \cong \frac{d N_{tu}}{d \mu_{CENTD}} \frac{\mu_{CENTD}}{N_{tu}}$$

or

$$\frac{\Delta N_{tu}}{N_{tu}} \cong K \frac{\Delta \mu_{CENTD}}{\mu_{CENTD}}$$

With empirical results he has tabulated values of K versus μ_{CENTD} and K versus N_{tu}.

As an example, using Kohlmayr's curves when μ_{CENTD} is measured too high by 2% and when K = -5.0, then N_{tu} as obtained by this method would be 10% too low.

Associated with the zero intercept technique are two distinct types of error. One results from the initial assumptions on which this technique

is based. These assumptions were discussed in Section 2. If errors are present in the results, they may be due to errors in the original assumptions. It is not possible to get, at this time, a quantitative value for this type of error or in fact to even verify that the technique used here is valid. The only factor which would substantiate the technique's validity is that for both heater systems used in the experiment the results in terms of N_{tu} were nearly identical. The second type of error is that associated with the physical data reduction, primarily the correct extrapolation of the response curve back to time zero, see Figure 17. This may be seen in the following development:

$$N_{tu} = -\ln(1 - t_f^*)$$

$$N_{tu} \pm \Delta N_{tu} = -\ln(1 - t_f^* \pm \Delta t_f^*)$$

$$\frac{e^{-N_{tu}} e^{\mp \Delta N_{tu}}}{e^{-N_{tu}}} = \frac{1 - t_f^* \pm \Delta t_f^*}{1 - t_f^*}$$

$$e^{\mp \Delta N_{tu}} = 1 \pm \frac{\Delta t_f^*}{1 - t_f^*}$$

or

$$\pm \Delta N_{tu} = \ln\left(1 \pm \frac{\Delta t_f^*}{1 - t_f^*}\right)$$

so that if $1 - t_f^* = .2$ corresponding to a value of $N_{tu} = 1.609$, and

$$\frac{\Delta t_f^*}{1 - t_f^*} = +.02 \qquad \text{or } 2\%$$

then

$$\Delta N_{tu} = +.0202 \qquad \text{or } 1.25\%$$

if $\frac{\Delta t_f^*}{1 - t_f^*} = -.02$ or -2%

then

$$\Delta N_{tu} = -.0198$$ or -1.2%.

8. Conclusions.

1. The present design of the new .001 inch diameter heaters was not found to be satisfactory due to their frequent and sometimes unexplained failures. No improvement of the results of the maximum slope and zero intercept tests was obtained using the smaller diameter wire heaters. No results were obtained with the new heaters for evaluation with the centroid technique, but it should be pointed out that for the centroid technique it is not necessary to have a step change in the inlet temperature so long as the actual change is known.

2. It would be extremely difficult to try and compare the three techniques used in this experiment on the basis of test results accuracy. The best that one can do at present is to compare the various experimental results with the predicted values based on the maximum slope technique evaluated at high values of N_{tu} ($N_{tu} > 5.0$). In this respect the maximum slope technique is unreliable for $N_{tu} < 3.5$. The centroid technique appears to have good results for $N_{tu} < 5$ to as low as .75 which was the minimum value tested in this experiment. For both the cores tested using the centroid technique the results were either the same as those predicted by the maximum slope technique or somewhat higher. The zero intercept method appears to be impractical for values of $N_{tu} > 2.5$ due to the larger differences associated with the logarithm of very small numbers. This might be better understood by looking at the governing equation in the zero intercept technique

$$N_{tu} = -\ln\left(1 - t_f^*(N_{tu}, 0)\right)$$

and noting that as the argument of the logarithmic term gets smaller the natural logarithm itself approaches negative infinity. Below the value of

$N_{tu} < 2.5$ the results were higher than predicted but were extremely consistent, that is, for different runs conducted at the same conditions the results were nearly identical.

From the standpoint of ease of evaluating, the zero intercept technique is very fast and simple to apply. Furthermore, in the method used in this experiment the zero intercept technique appears to be insensitive to slight deviations from a step temperature change. On the other hand the results of the centroid technique rely entirely upon how well the so called "deviation from step" change of the fluid's upstream temperature is known.

The centroid technique is much more time consuming to use and in view of the fact that its results are based on a considerable portion of the fluid temperature response trace it is more subject to errors caused by sudden fluctuations in the ambient conditions, for in the zero intercept technique only the very first part of the trace is of interest. Based upon the above conclusions the following table is recommended as a guide in determining which of the aforementioned techniques should be used for a given test range.

N_{tu} Range	Technique
$3.5 < N_{tu}$	Maximum Slope
$2.5 < N_{tu} < 3.5$	Centroid Technique
$N_{tu} < 2.5$	Zero Intercept Technique

9. Recommendations for Further Study.

It is recommended that an attempt be made to determine both experimentally and analytically the effects of deviations from experimental assumptions such as constant fluid properties and the convective heat transfer coefficient on the results using the different techniques including the cyclic testing technique.

10. Bibliography.

1. American Society of Mechanical Engineers., Power Test Code Supplements, Instruments and Apparatus, PTC-19.5; 4, Flow Measurements, Chap. 4, New York: ASME 1959.

2. Ball, Stuart F., "Experimental Determination of Heat Transfer and Flow Friction Characteristics for Several Plate Fin Type Compact Heat Exchanger Surfaces," Master's Degree Thesis, Naval Postgraduate School, Monterey, California, 1966.

3. Bannon, John M., "An Experimental Determination of Heat Transfer and Flow Friction Characteristics of Perforated Material For Compact Heat Exchanger Surfaces," Master's Degree Thesis, Naval Postgraduate School, Monterey, California, 1964.

4. Bell, J. C. and Katz, E. F., "A Method for Measuring Surface Heat Transfer Using Cyclic Temperature Variations," Heat Transfer and Fluid Mechanics Institute, Berkeley, California, 1949.

5. Hausen, H., Z. Math, Mech. 9, page 173, 1929.

6. Howard, C. P., "The Single Blow Problem Including The Effects of Longitudinal Conduction," ASME paper number 64-GTP-11, 1964.

7. Howard, C. P., "Heat-Transfer and Flow Friction Characteristics of Skewed-Passage and Glass-Ceramic Heat-Transfer Surfaces," TR No. 59, Department of Mechanical Engineering, Stanford University, Stanford, California, October 1963.

8. Kays, W. M., and London, A. L., Compact Heat Exchangers, Second Edition, McGraw-Hill Book Co., Inc., New York, 1964.

9. Kohlmayr, G. F., "Exact Maximum Slopes for Transient Matrix Heat Transfer Testing," Pratt & Whitney Aircraft, Report PWA-2641.

10. Kohlmayr, G. F., "Analytical Solution of the Single-Blow Problem by a Double La Place Transform Method," Pratt & Whitney Aircraft, Report PWA-3158, July 1967.

11. Kohlmayr, G. F., "An Indirect Curve Matching Method for Transient Matrix Heat-Transfer Testing in the Low N_{tu} Range," Pratt & Whitney Aircraft, Report PWA-3207, September 1967.

12. Kohlmayr, G. F., "Extension of the Maximum Slope Method to Arbitrary Upstream Fluid Temperature Changes," Pratt & Whitney Aircraft, Report PWA-3228.

13. Locke, G. L., "Heat Transfer and Flow Friction Characteristics of Porous Solids," TR. No. 10, Department of Mechanical Engineering, Stanford University, Stanford, California, 1 June 1950.

14. Murdock, J. W., "Tables for Interpolation and Extrapolation of ASME Coefficients for Square-Edged Concentric Orifices," ASME Paper No. 64-WA/FM-6.

15. Piersall, C. H., "Experimental Evaluation of Several High Performance Surfaces for Compact Heat Exchangers," Master's Degree Thesis, Naval Postgraduate School, Monterey, California, 1965.

16. Traister, R. E., "Experimental Evaluation of Heat Transfer and Flow Friction Characteristics of Several Compact Heat Exchanger Surfaces Utilizing the Single Blow and Cyclic Methods," Master's Degree Thesis, Naval Postgraduate School, Monterey, California, 1967.

17. Wheeler, A. J., "Single-Blow Transient Testing of Matrix-Type Heat Exchanger Surfaces At Low Values of N_{tu}," TR. No. 68, Department of Mechanical Engineering, Stanford University, Stanford, California, May 1968.

18. Trost, H. J., Jr., "The Use of The Analog Computer With the Single Blow Transient Testing Technique For Compact Heat Exchanger Surfaces," Master's Degree Thesis, Naval Postgraduate School, Monterey, California, September 1967.

APPENDIX A

Description of Equipment

Air Supply.

The working fluid for the experiment is air drawn through the test equipment by a 30 HP, multi-stage Spencer Turbo-Compressor, which is rated at 550 cfm operating on a 220 V a.c. power supply see Figure 3.

Flow Measuring System.

Flow measurement was accomplished with an ASME standard orifice section. Pressure taps were located d and d/2 diameters upstream and downstream respectively from the orifice. Thin concentric orifices with throat diameters of .775, 1.232, 1.540, and 2.310 inches were used.

Heater System.

Two different heater systems were used. One system utilized a .0031 inch diameter nichrome wire as the heating element, and the other .001 inch nichrome wire. Both systems were designed to give the same nominal resistance for a given number of heater switches.

The .0031 inch system,(Figure 18A), consisted of 14 separate bakelite frames, each wound with two parallel-connected heater elements. Each pair of heaters was controlled by an individual switch, which in turn was wired in parallel with the other heater switches. All were controlled by one master switch.

The .0010 inch system (Figure 18B) consisted of the same number of bakelite frames, with each frame containing six heater elements connected in parallel. The number of heaters and voltage could be varied to achieve approximately a 20°F. temperature change for any given flow rate.

Matrix Holder and Test Section.

The matrix holder and test section (Figure 4) were both constructed

of polyethylene plastic. The matrix holder is a drawer which slides into the test section. A removable frame on the side of the holder allows for the insertion of the matrix. The flow channel is 3-1/16 inches by 3-1/16 inches, and can hold matrices up to 3 inches long. The matrix is held snugly in place by styrofoam insulation. On the downstream side of the holder is a plate containing the thermocouples used to measure t_3. The test section into which the holder slides contains the heaters, pressure taps, and the thermocouple set downstream from the heaters, which measures t_2.

Inlet Cone and Flow Straightener

This section was designed and tested by Piersall [15], and it provided a uniform velocity profile to the air entering the matrix.

Pressure Measuring System

Pressure taps are located in the test section upstream and downstream from the matrix holder, (see Figure 5). Two other taps are located at the orifice section. Each pressure tap is connected by flexible tubing to its corresponding manometer and/or draft gage. The following instruments were used interchangeably, depending upon the flow rate:

1. Ellison Draft Gage Company, 0-3 in. inclined gage
2. Ellison Draft Gage Company, 10 in. manometer
3. Ellison Draft Gage Company, 20 in. manometer
4. Merriman Instrument Company, 120 in. manometer
5. Precision Thermometer and Instrument Company, mercury barometer

Temperature Measuring System

Temperatures in the system are measured at four locations: (See Figure 5)inlet to the system (t_1), downstream from the heaters (t_2),

downstream from the matrix (t_3), and at the orifice (t_0).

Temperature t_1 is measured by two different sets of 30 gage iron-constantan thermocouples, which were made by Traister [16]. Each set consists of 5 thermocouples connected in series. Each thermocouple is individually wrapped in teflon tape to prevent shorting. All ten are contained in an open-faced aluminum tube mounted in a frame at the exit of the inlet cone. The aluminum tube shielded against radiation from the heaters.

Temperature t_2 was measured by a set of five .001 inch diameter iron-constantan thermocouples connected in series. The output of these was bucked against one of the sets measuring t_1 so that the output of the two sets measured (t_2-t_1).

Temperature t_3 was measured in the same manner as t_2 and the output bucked against the other set measuring t_1 so that the output measured (t_3-t_1). The outputs (t_3-t_1) and (t_2-t_1) could be recorded separately or bucked against each other to give (t_3-t_2). The desired outputs were then led into an Astrodata Model 886 Wideband Differential D. C. Amplifier, where they were amplified 100:1. From there the signal was led into a Brush Mark 280 Strip Chart Recorder.

Temperature t_0 was measured by a 30 gage copper-constantan thermocouple referenced to an ice junction. The output was read on a Leeds & Northrup Millivolt Potentiometer.

Heater Power.

The power to the heaters was supplied from the 250 V. D. C. source in the laboratory. The actual voltage was controlled both at the supply panel and at the apparatus by means of a 50 Ω wound resistor.

APPENDIX B

Data Reduction Relationships

(1) The following is a summary of the data reduction relationships used in calculating N_{tu} by the maximum slope technique.

Geometry.

Three geometric parameters may be used to define compact heat transfer surfaces. This allows for the comparison of different matrices.

1. Hydraulic Diameter

$$D_H = 4r_h = \frac{4x \text{ free flow area}}{\text{heat transfer area}} \tag{B-1}$$

2. Porosity

$$p = \frac{\text{free flow area}}{\text{frontal area}} = \frac{A_c}{A_{fr}} \tag{B-2}$$

3. Area Compactness

$$\beta = \frac{\text{heat transfer area}}{\text{matrix volume}} = \frac{A}{A_{fr}L} \tag{B-3}$$

Dividing (B-2) by (B-3)

$$r_h = p/\beta \tag{B-4}$$

Mass Rate of Fluid Flow

The mass flow rate, $\dot{m}$, is calculated from ASME Power Test Code [1] as modified by Murdock [14] by the following equation:

$$\dot{m} = 359\, K d_o^2 F_a Y \sqrt{P_o \gamma} \tag{B-5}$$

where

$K = \frac{C}{\sqrt{1 - \bar{\beta}^4}}$ flow coefficient including velocity of approach

C = orofice coefficient of discharge [14]

$\bar{\beta}$ = ratio of orifice diameter to pipe diameter

d_o = orifice diameter in inches

F_a = thermal expansion factor

γ = P/RT the specific weight of fluid flowing, assuming a perfect gas (lbf/ft^3)

Y = expansion factor

P = absolute static pressure at orifice (lbf/sq ft)

R = gas constant for air: 53.35 (ft-lbf/lbm°R)

T = absolute temperature at orifice (deg R)

ΔP_o = pressure drop across the orifice in inches H_2O

Substituting the expressions for K and γ in equation (B-5) yields:

$$\dot{m} = 359 \frac{C}{\sqrt{1-\bar{\beta}^4}} d_o^2 F_a Y \sqrt{\frac{\Delta P_o P}{RT}} \qquad \text{(B-6)}$$

From [1] Fig. 40A

$$Y = 1 - (0.41 + 0.35\bar{\beta}^4)\frac{X}{k}$$

k = 1.4 for air, ratio c_p/c_v

Also, from [1], Fig. 38

F_a = 1.0

P = $(P_{atm} - P_o/13.6)(0.4912*144)$ lbf/ft^2

P_{atm} = local atmospheric pressure in inches Hg

P_o = static pressure upstream of the orifice plate in inches Hg

Making the above substitution in (B-6) with the constants necessary to be dimensionally consistent yields:

$$\dot{m} = 589.81 (C/\sqrt{1-\bar{\beta}^4}) d_o^2 \left[1 - (.41 + .035\bar{\beta}^4)\right] \frac{\Delta P_o}{\left(P_{atm} - \frac{P_o}{13.6}\right)} \frac{1}{99.02} \left[\frac{\Delta P_o (P_{atm} - P_o/13.6)}{t_o + 459.7}\right]^{1/2} \qquad \text{(B-7)}$$

Reynolds Number

Reynolds Number is defined as:

$$N_{Re} = \frac{D_H G}{\bar{\mu}} \tag{B-8}$$

where G, the mass flow velocity = $\dot{m}/A_c = \dot{m}/pA_{fr}$ (B-9)

and $\bar{\mu}$ is the fluid viscosity.

Substituting:

$$N_{Re} = \dot{m} D_H / \bar{\mu} A_{fr} P = 4\dot{m}/\bar{\mu} A_{fr} \bar{B}$$

or

$$N_{Re} = 4\dot{m}L / A\bar{\mu} \tag{B-10}$$

Maximum Slope

The maximum slope of the downstream cooling curve (t_3-t_1) is a unique function of N_{tu} [13] and λ [6].

$$\left[\frac{d\left(\frac{t_3-t_i}{t_1-t_i}\right)}{d\left(\tau/N_{tu}\right)}\right]_{max} = \phi(N_{tu}, \lambda)$$

τ, N_{tu} and λ have been previously defined, but for convenience are restated:

$$\tau = \frac{hA}{W_s c_s}\theta, \quad N_{tu} = \frac{hA}{\dot{m} c_f} \quad \text{and} \quad \lambda = \frac{K_s A_s}{\dot{m} c_f L}$$

the new temperature introduced is t_i and is equal to the temperature of both the solid and the fluid prior to cooling.

Therefore:

$$\tau / N_{tu} = (\dot{m} c_f / W_s c_s)\theta$$

and

$$d(\tau/N_{tu}) = (\dot{m}c_f/W_s c_s)\,d\theta \tag{B-11}$$

letting:

$C_f = \dot{m}c_f$ (Fluid stream thermal capacity rate)

and

$C_s = W_s c_s$ (Matrix heat capacity)

equation (B-11) becomes,

$$d(\tau/N_{tu}) = (C_f/C_s)\,d\theta$$

Furthermore

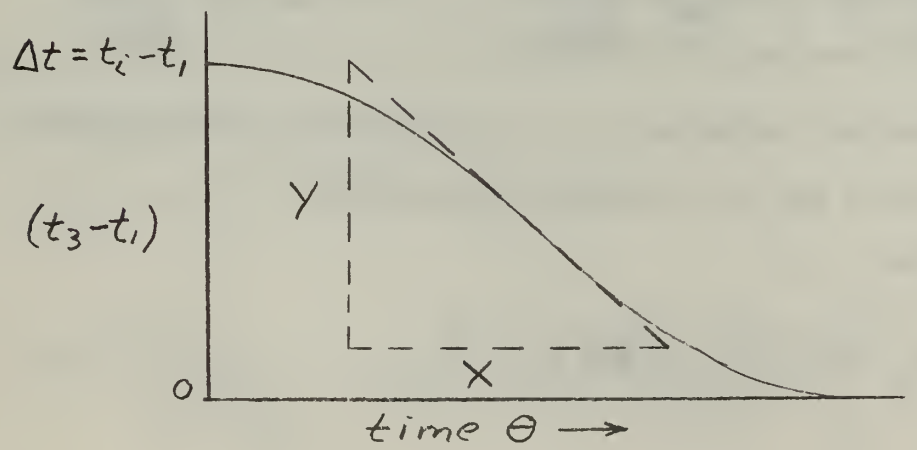
$$\frac{t_3 - t_i}{t_1 - t_i} = \frac{t_3 - t_1}{t_1 - t_i} + 1$$

whose derivative is:

$$d\left(\frac{t_3 - t_i}{t_1 - t_i}\right) = \frac{1}{t_3 - t_i}\,d(t_3 - t_1) \tag{B-12}$$

combining equations (B-11) and (B-12) yields:

$$\left[\frac{d\left(\frac{t_3 - t_i}{t_1 - t_i}\right)}{d(\tau/N_{tu})}\right]_{MAX} = \frac{W_s c_f}{\dot{m} c_f}\,\frac{1}{t_1 - t_i}\,\frac{d(t_3 - t_1)}{d\theta} \tag{B-13}$$



From the above sketch of the downstream temperature response curve:

$$\left[\frac{d(t_3-t_1)}{d\Theta}\right]_{MAX} = Y/X$$

X/ chart speed $= d\Theta$

$d(t_3-t_1) = Y$

$t_i-t_1 = \Delta t$

combining with the ratio of,

$$\frac{\text{matrix capacity}}{\text{flow stream capacity rate}} = \frac{C_s}{C_f} \quad (1/sec)$$

and equation (B-13)

$$\left[\frac{d\left(\frac{t_3-t_i}{t_1-t_i}\right)}{d(\tau/N_{tu})}\right]_{MAX} = \frac{C_s}{C_f}\frac{1}{\Delta t}\frac{Y}{X}\ \text{Chart speed} \qquad \text{(B-14)}$$

This value of maximum slope and λ are then used to enter Table III or Figure 14 or 15 to get the corresponding value of N_{tu}.

(2) Centroidal Technique

For the centroidal technique the recording trace of (t_3-t_2) is used. Two methods are actually involved in utilizing this trace. One method is to copy the trace physically with carbon paper on to a thin piece of cardboard. Then the trace copy is cut out, and by means of a "plumb-line" attached to a pivot, which allows the trace to swing free, the line passing through the pivot point and the center of mass is determined. This is done for several points (at least 3) and the intersection of the different lines is the centroid of the area under the response curve.

These lines are shown in Figure 16. Ideally all lines will intersect at the same place, however, this is not the case in actuality due to errors in manipulation.

An alternate method is also used to find the centroid of the function (t_3-t_2). This involves the use of a computer program, which when fed actual curve data (normalized) computes the centroid. This is done in the absence of an apparatus which could convert directly the temperature response to information useable by the digital computer, such as a paper tape puncher.

Once μ_{CENTD} is determined from the trace of (t_3-t_2) it is necessary to compute I(g) in the manner described in Appendix C. This value of I(g) is then used to determine μ_o. Recall Equation (14)

$$\mu_{CENTO} \cong \mu_o + .99\, I(g) \pm .01$$

or

$$\mu_o \cong \mu_{CENTO} - .99\, I(g) \mp .01$$

Once μ_o is determined, Kohlmayr's curve of N_{tu} vs. μ_o, Figure 1, may then be entered to give N_{tu}.

(3) Zero Intercept Technique.

To interpret the physical data, i.e., the recorded trace of (t_3-t_1), which represents t_f, in the manner described in Section 3, of this report:

(i) Extrapolate by means of a French curve the response curve (t_3-t_1) from some position on the trace where the transient response of the heaters has died out, back to the vertical line passing through the point $\mu = 0$. This point would be the position where the first change in temperature was detected by the thermocouples and is referred to as $(t_3-t_1)_o$ or $t_f\,(N_{tu}, O)$, Figure 2B.

(ii) Record the value of (t_3-t_1) at the intersection of

the time zero line and the extrapolated response curve, also record the value of (t_3-t_1) at the time just prior to the heaters being deenergerized. This temperature is referred to as $(t_3-t_1)_{max}$.

(iii) N_{tu} is then equal to,

$$N_{tu} = -\ln(1- (t_3-t_1)_0/(t_3-t_1)_{max})$$

which was developed in Section 3, as,

$$N_{tu} = -\ln(1-t_f^*(N_{tu},0))$$

APPENDIX C

To determine the transient response of the NPS facility for different heater sets, runs were conducted in which the temperature difference (t_2-t_1) was recorded as a function of time. This temperature difference, which was previously called "upstream temperature" is the difference in temperature of the air entering the test rig and the air leaving the heaters.

Analytical determination of the heater time constant is straightforward and presents no difficulty based strictly on the analysis of a cylinder in cross flow. The analytical determination of the thermocouple time constant is more difficult and requires some judgment. Since the thermocouples are constructed of .001 inch diameter wire, it is not possible to describe precisely and mathematically the geometry of their junction. In the construction of the thermocouples the two different wires used crossed, at an angle approaching 180 degrees, and arc-welded at the junction. Therefore, the junction was neither spherical nor cylindrical (which is the case when the wires are butt-welded). For this reason the model of the junction was arbitrarily chosen to be spherical and calculations were based on a spherical junction .002 inches in diameter. On this basis it was determined that the time constant of the .003 inch heaters was nearly three times greater than the time constant of the thermocouples, while the time constant of the .001 inch heaters was approximately two-thirds that of the thermocouples.

Since the response of the heater-thermocouple circuit would be the sum of at least two exponential terms, which would be difficult to separate experimentally, the terms have been treated here as one exponential term, which is a good approximation of the actual system response

if one neglects the initial points on the response curve. From the normalized temperature response curves the following empirical relations were developed:

where θ = time in seconds and

θ_H is the heater time constant in seconds

$$\frac{t_2 - t_1}{(t_2 - t_1)_{MAX}} = e^{-\theta/\theta_H} \qquad \text{(C-1)}$$

$$\log\left[\frac{(t_2 - t_1)}{(t_2 - t_1)_{MAX}}\right] = -\frac{\theta}{\theta_H} \log e \qquad \text{(C-2)}$$

$$\theta_H = \frac{-\theta}{\log\left[\frac{(t_2 - t_1)}{(t_2 - t_1)_{MAX}}\right]} \log e \qquad \text{(C-3)}$$

where the value of $\dfrac{-\theta}{\log\left[\dfrac{(t_2-t_1)}{(t_2-t_1)\text{max.}}\right]}$ is the reciprocal of the slope of the temperature response curve.

The heater time constant was then plotted against mass flow rate ($\dot{m}$). From these curves the following relationships were obtained:

$$\log \theta_H = -a \log \dot{m} + \log c \qquad \text{where } a \text{ \& } c \text{ are constants} \qquad \text{(C-4)}$$

$$\theta_H = c\,\dot{m}^{-a} \qquad \text{(C-5)}$$

Since the centroid technique makes use of the deviation from step defined

as $$I(g) = \int_0^\infty g(\mu)\, d\mu \qquad \text{(C-6)}$$

and since $\mu \cong \alpha\theta$ and $d\mu = \alpha\, d\theta$

then $$g(\mu) = g(\theta) = e^{-\theta/\theta_H} = e^{-\mu/\alpha\theta_H} \qquad \text{(C-7)}$$

$$I(g) = \int_0^\infty e^{-\mu/\alpha\theta_H}\, d\mu = \alpha\,\theta_H \qquad \text{(C-8)}$$

where again $\alpha = \dfrac{\dot{m} c_f}{W_s c_s}$ $= \dot{m}^*$ constant (for any given core)

Therefore to determine I(g) for a particular run, enter the curve of θ_H vs. $\dot{m}$ (Figure 12) with appropriate $\dot{m}$. Note that this curve is independent of the matrix used in the run. Then multiply θ_H by the appropriate α to obtain I(g) used in centroid technique. Figure 12 shows the experimental values of θ_H vs. $\dot{m}$ plus the theoretical plots of heater and thermocouple transient response for both sets of heaters.

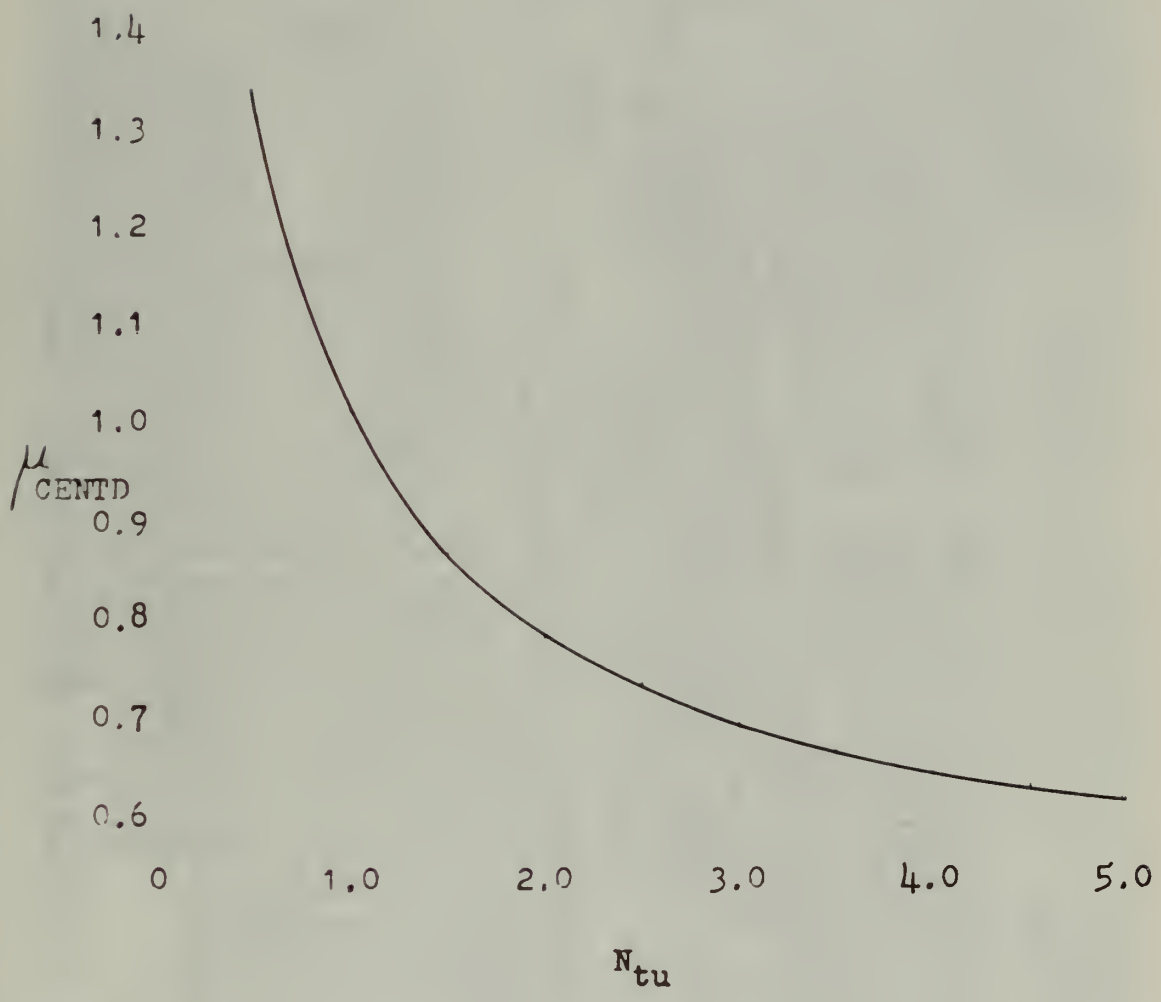


Figure 1. μ_{CENTD} Versus N_{tu}

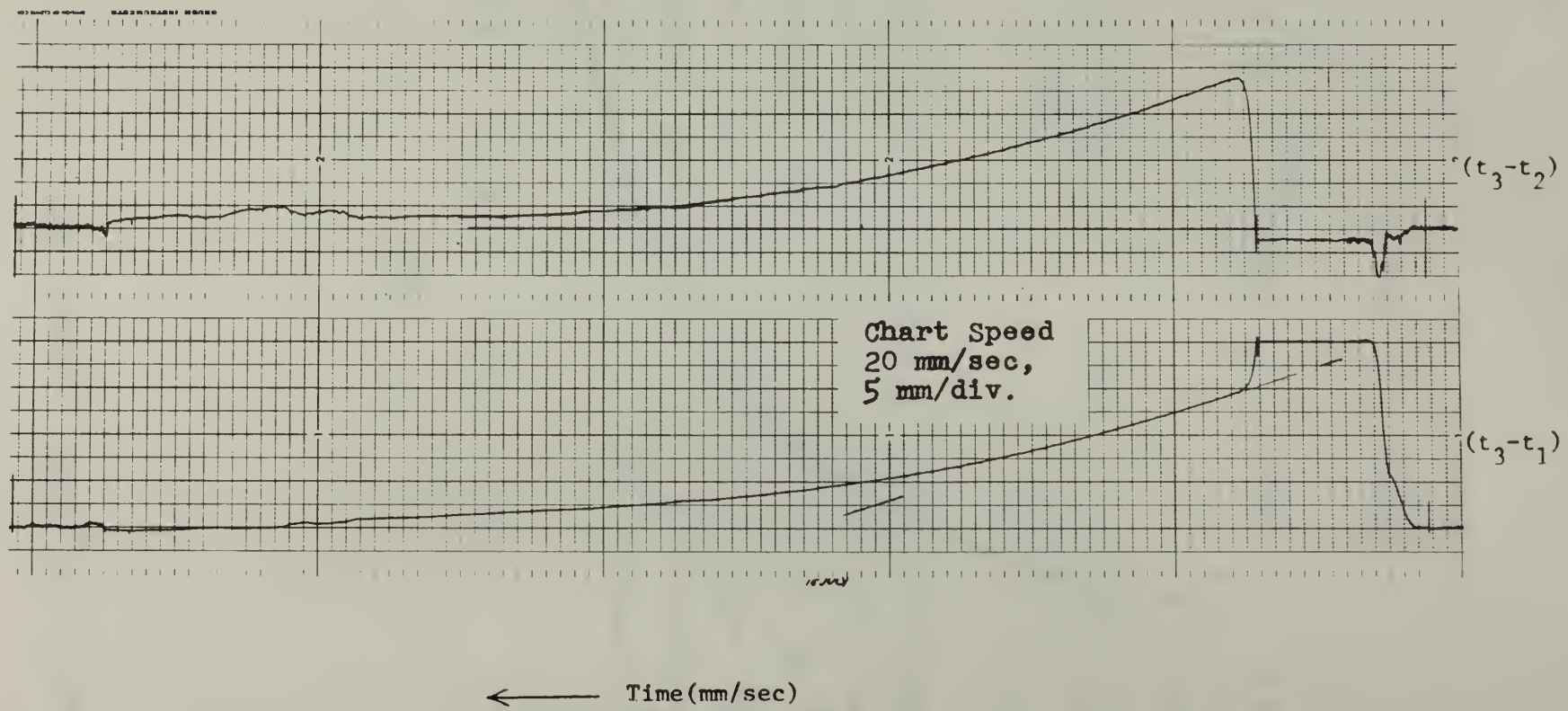


Figure 2. Sample Recording of Temperature Responses

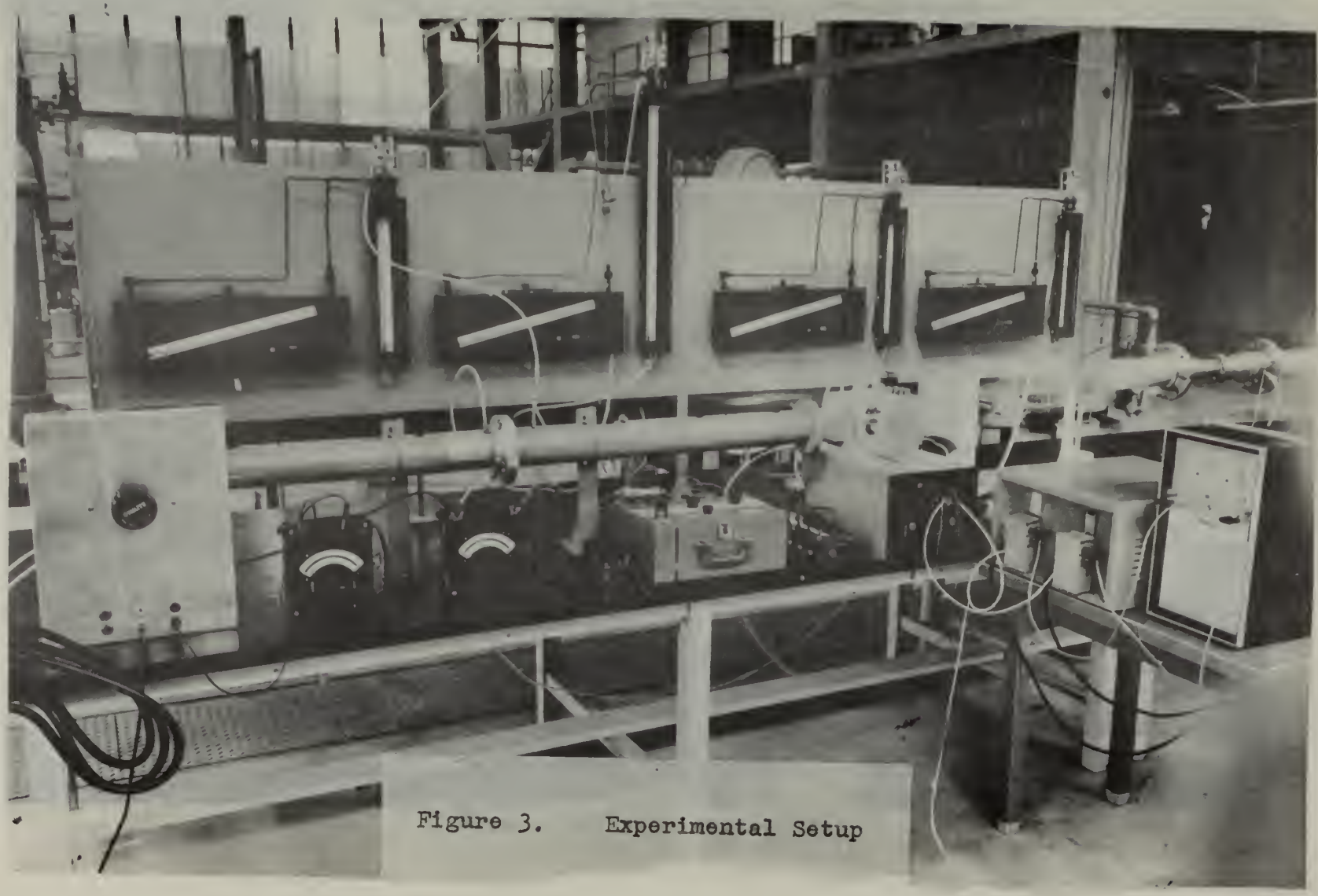


Figure 3. Experimental Setup

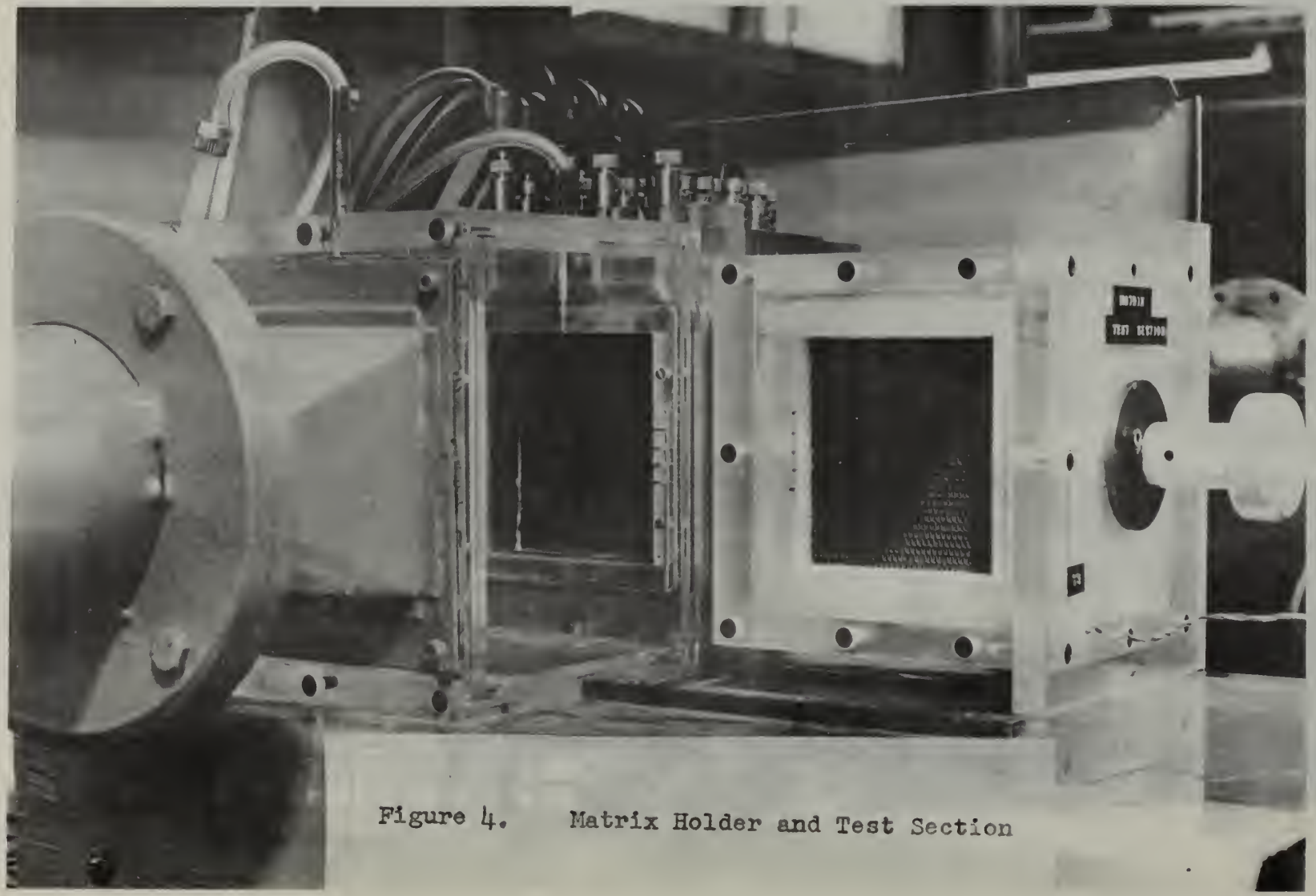


Figure 4. Matrix Holder and Test Section

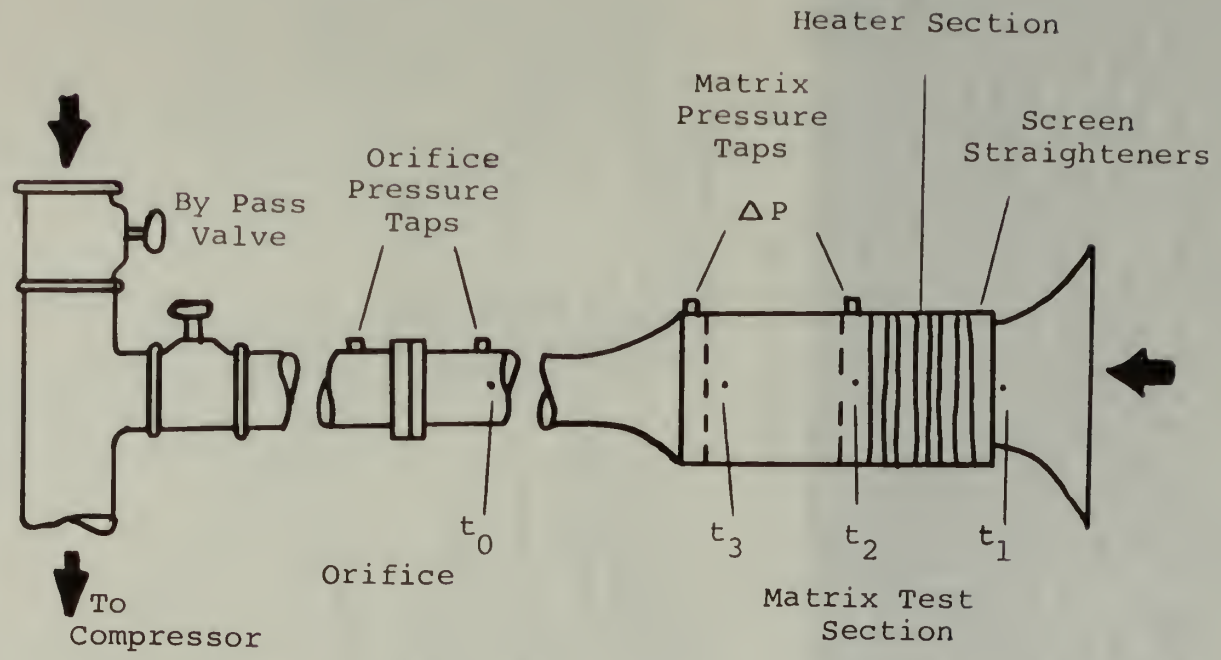
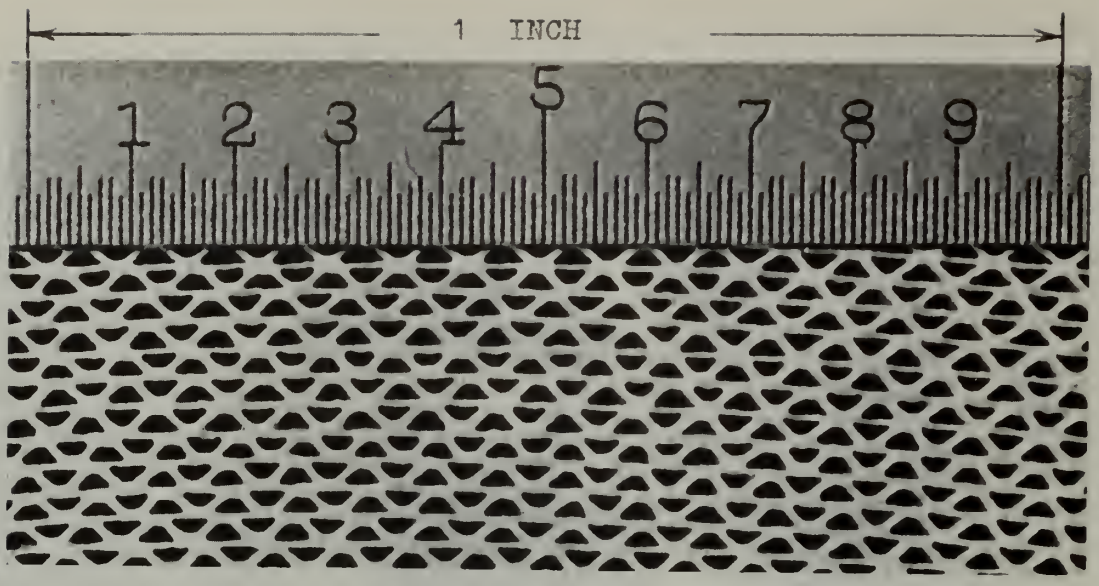


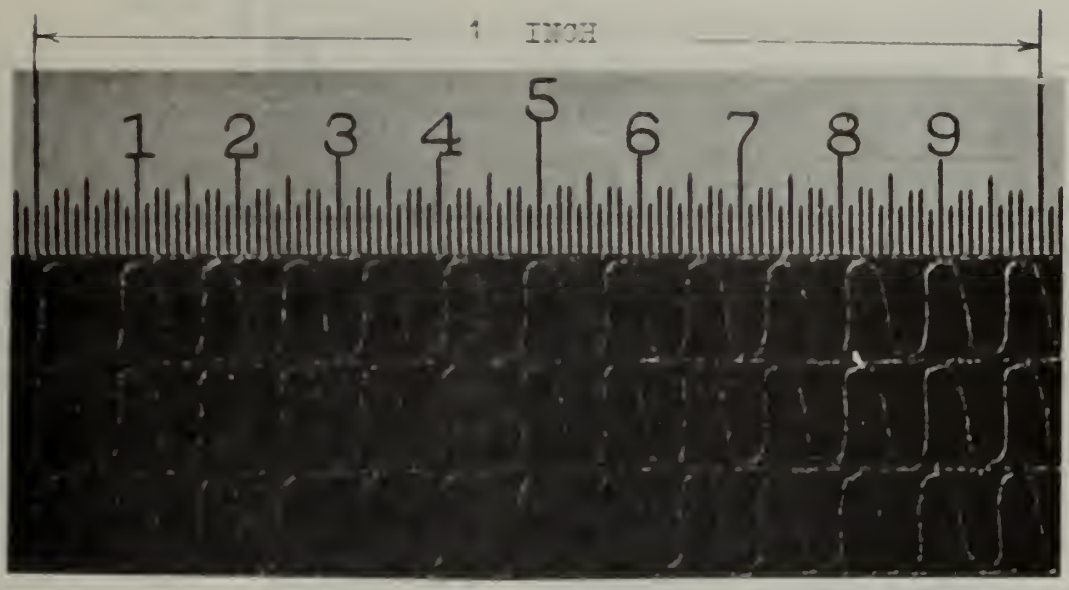
Figure 5. Schematic of Test Apparatus



Cercor T20-38

Matrix Material	Glass-ceramic	
Specific Heat	Btu/lbm deg F	.20
Thermal Conductivity	Btu/hr ft deg F	.034
Material Thickness	inches	.005
Total Heat Transfer Area	sq ft	17.81
Frontal Area	sq ft	.07124
Heat Conduction Area	sq ft	.02657
Free Flow Area	sq ft	.04467
Matrix Flow Length	ft	.16667
Matrix Density	lbm/cu ft	37.3
Compactness	sq ft/cu ft	1500.
Porosity		.62700
Hydraulic Diameter	ft	.00160

Figure 6. Geometric and Physical Properties of Core T 20-38



Solar 4

Matrix Material	430 Stainless Steel	
Specific Heat	Btu/lbm deg F	.11
Thermal Conductivity	Btu/hr ft deg F	12.8
Material Thickness	inches	.005
Total Heat Transfer Area	sq ft	14.27494
Frontal Area	sq ft	.01713
Heat Conduction Area	sq ft	.01229
Free Flow Area	sq ft	.05484
Matrix Flow Length	ft	.24417
Matrix Volume	cu ft	.01628
Matrix Density	lbm/cu ft	88.5918
Compactness	sq ft/cu ft	870.969
Porosity		.81690
Hydraulic Diameter	ft	.00375168

Figure 7. Geometric and Physical Properties of Core Solar 4

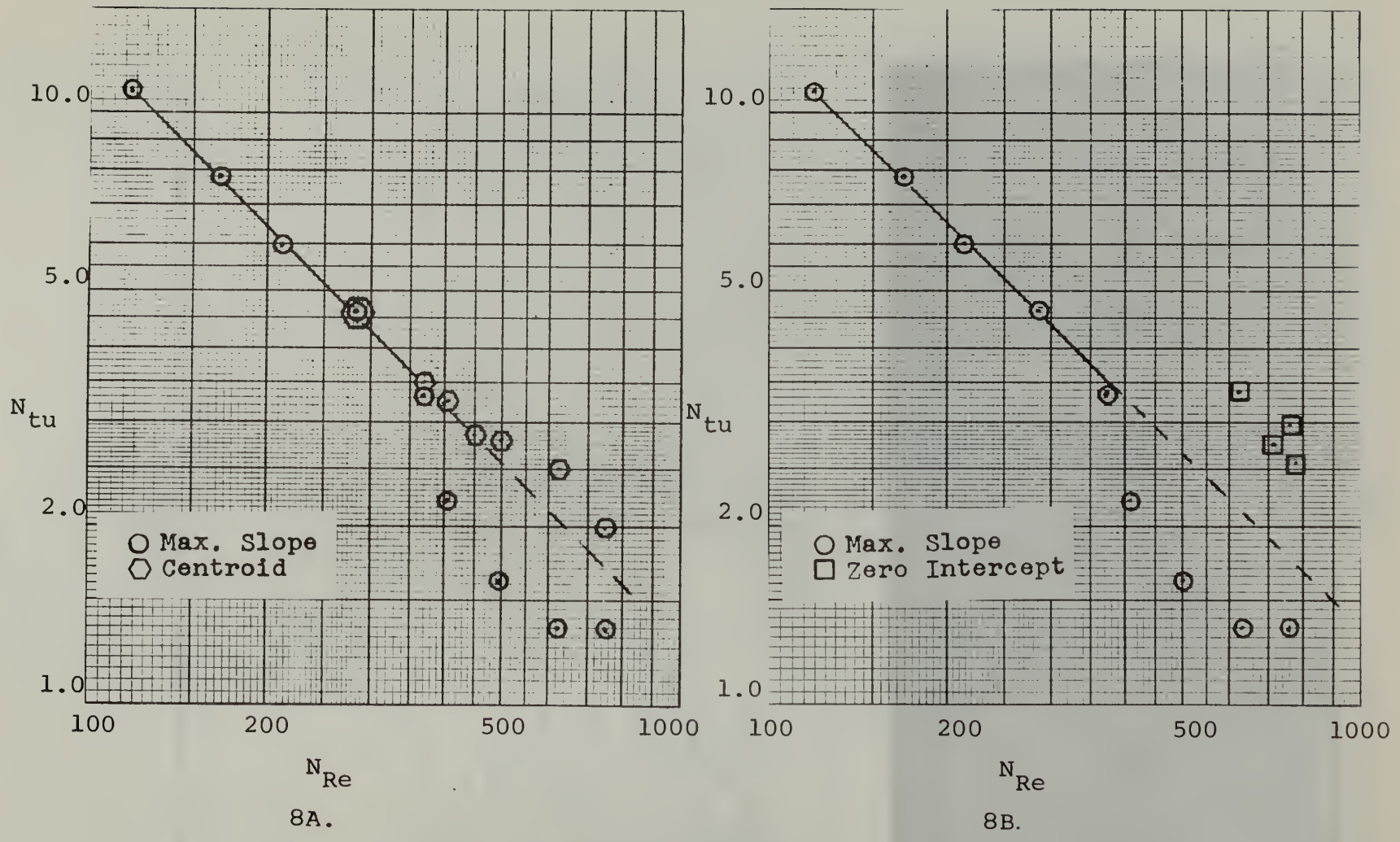


Figure 8. Core T20-38 Test Results

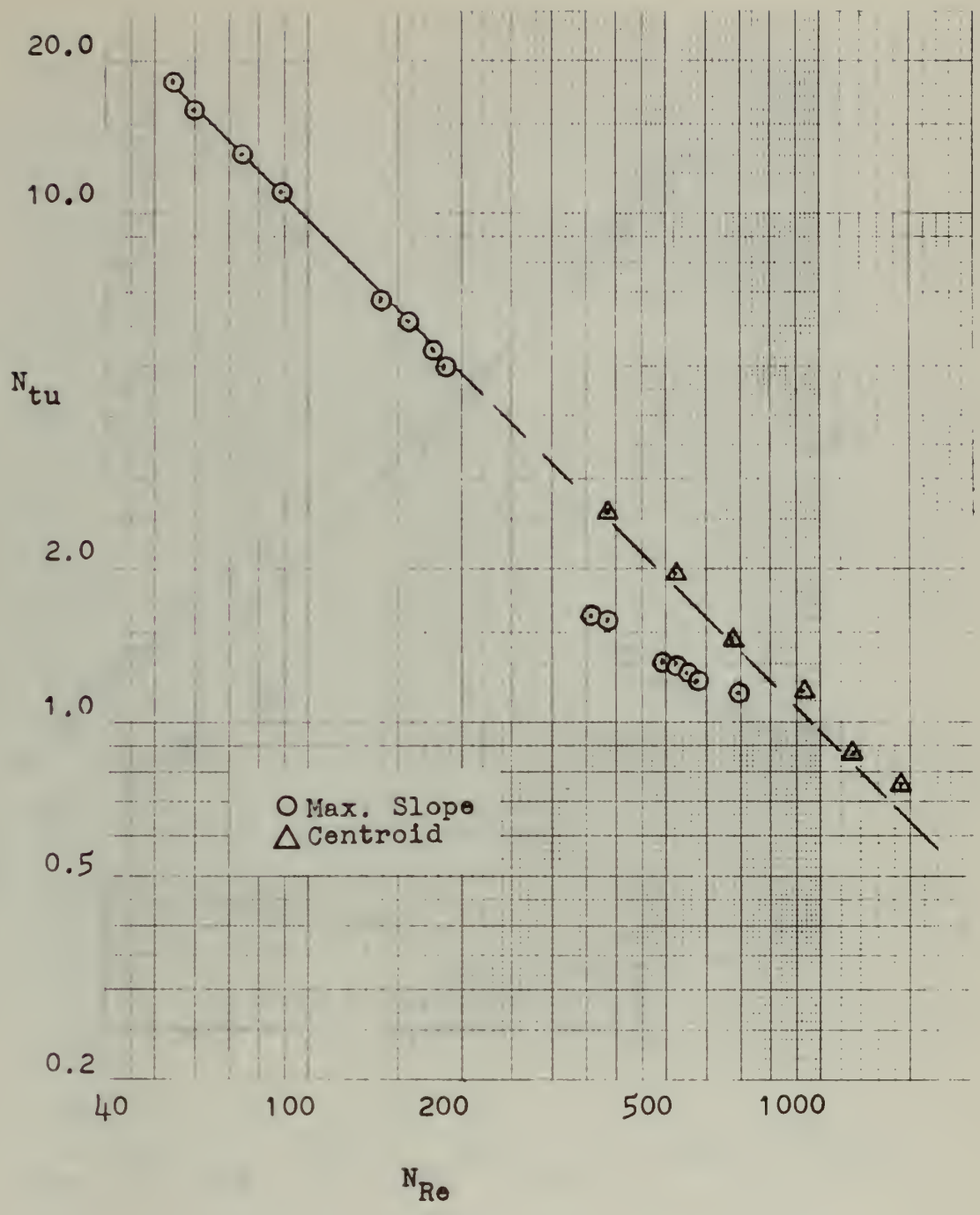


Figure 9. Core Solar 4 Test Results

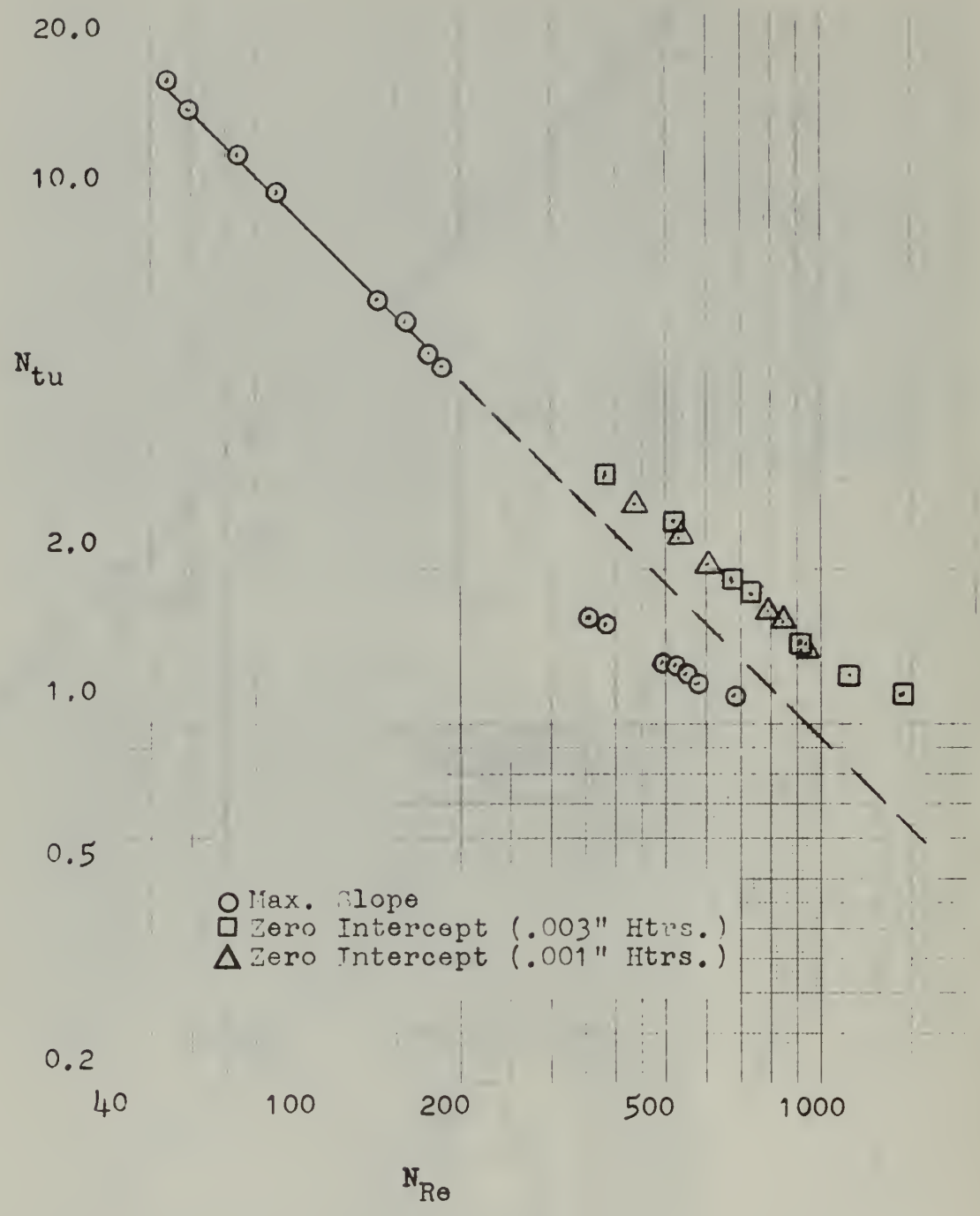


Figure 10. Core Solar 4 Test Results

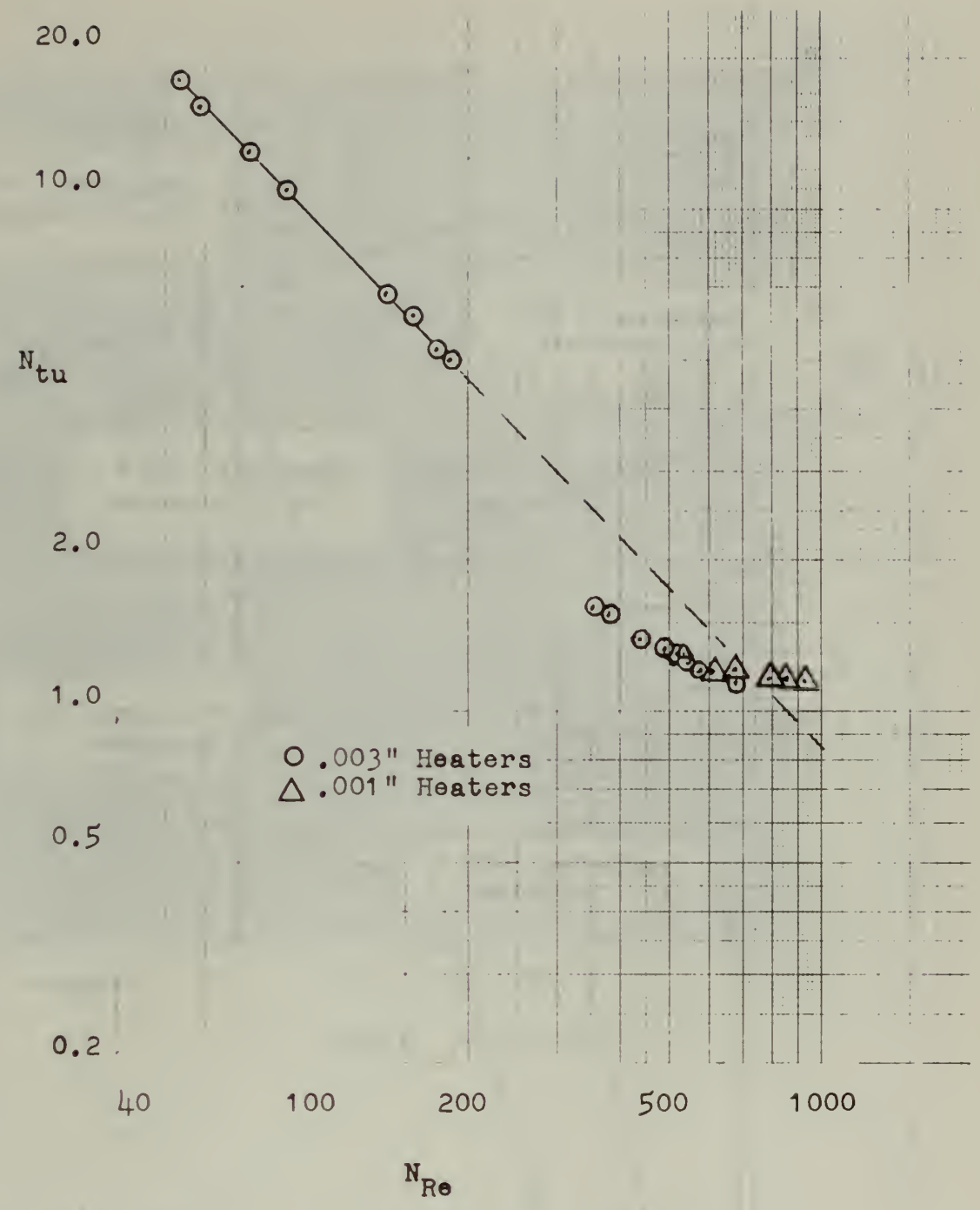


Figure 11. Comparison of Maximum Slope Test Results of Core Solar 4, With .003" and .001" Heaters

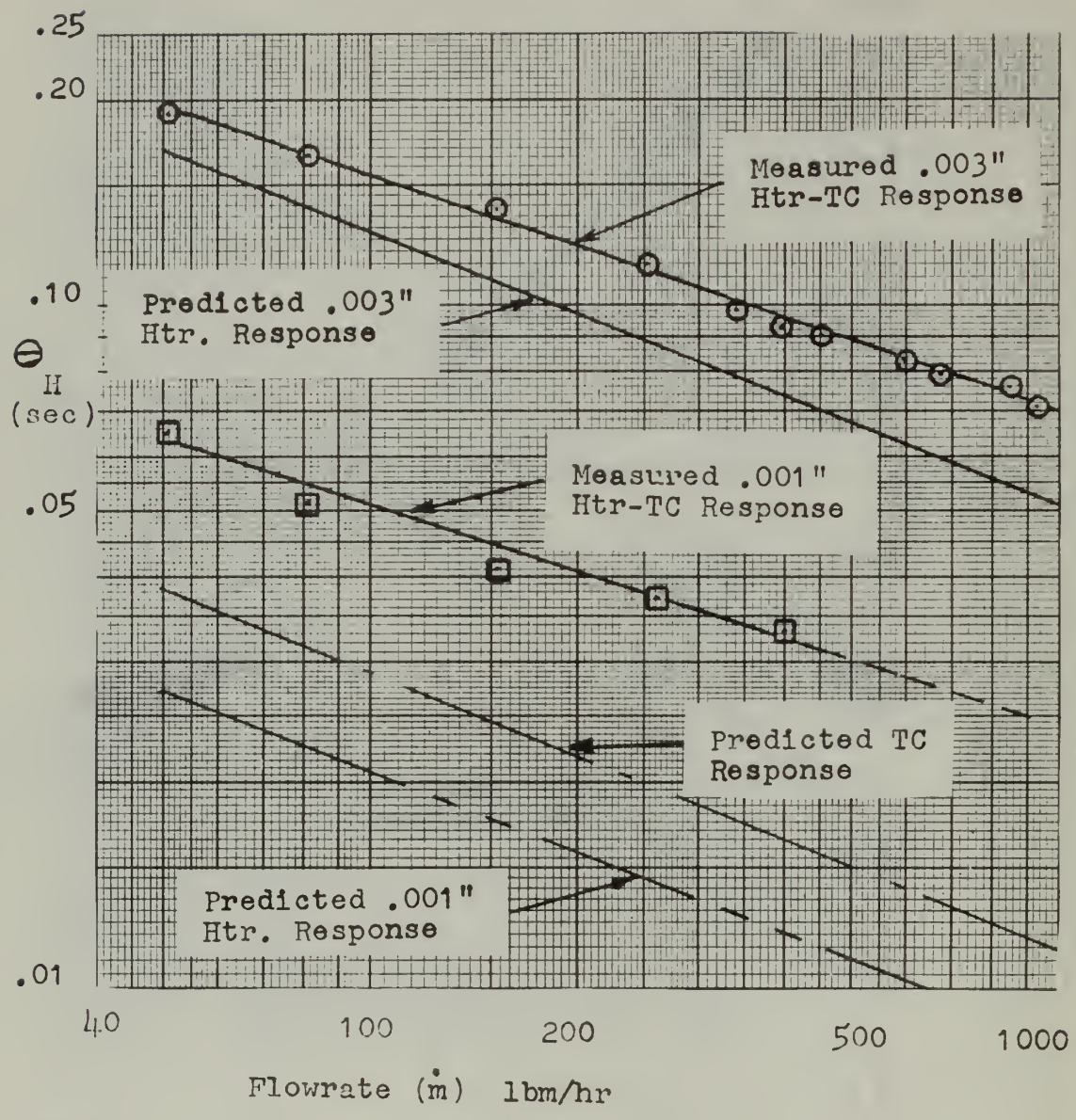


Figure 12. Heater Time Constant Versus Flowrate

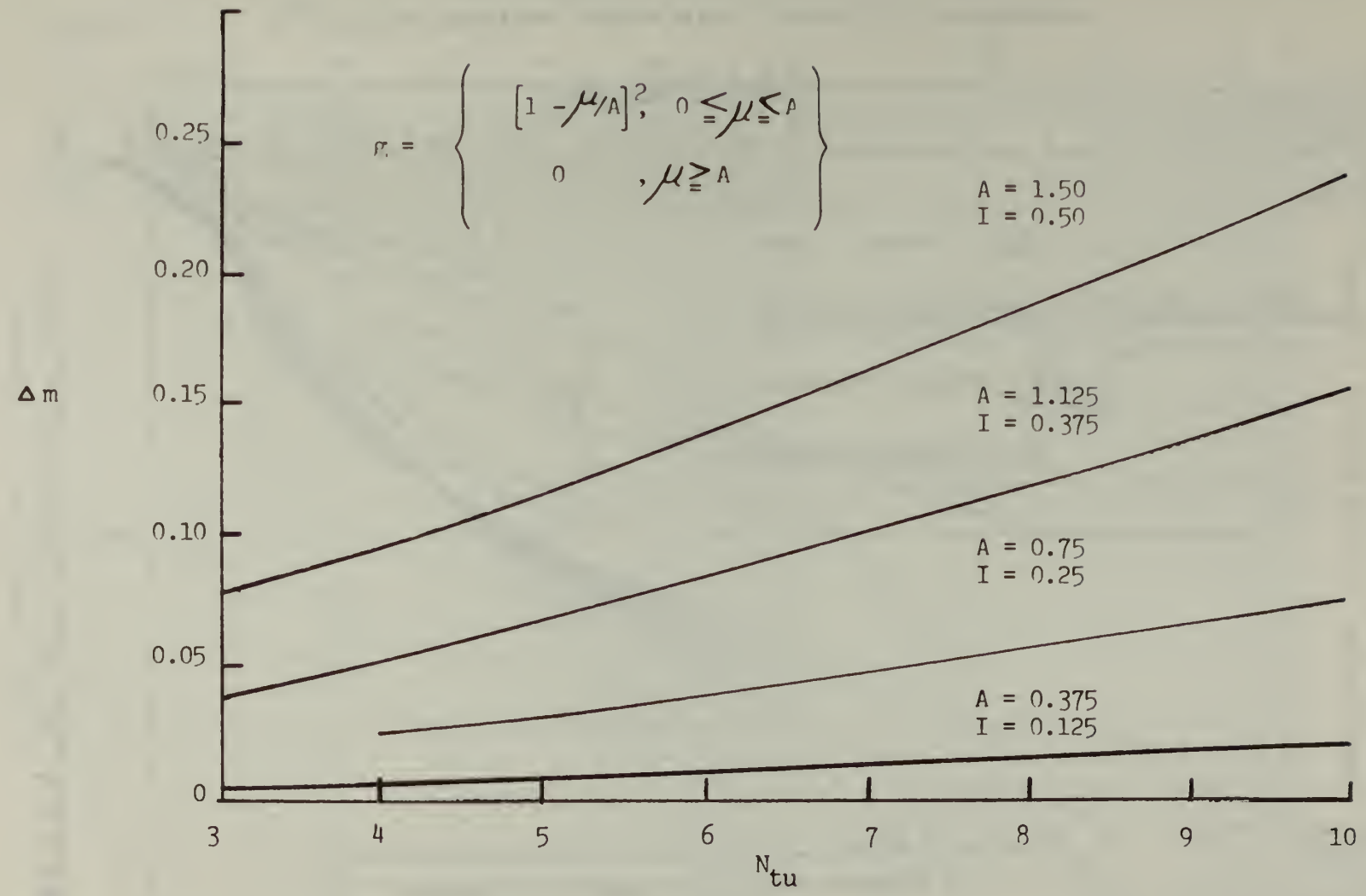


Figure 13. Error in Maximum Slope Due to Deviation From Step

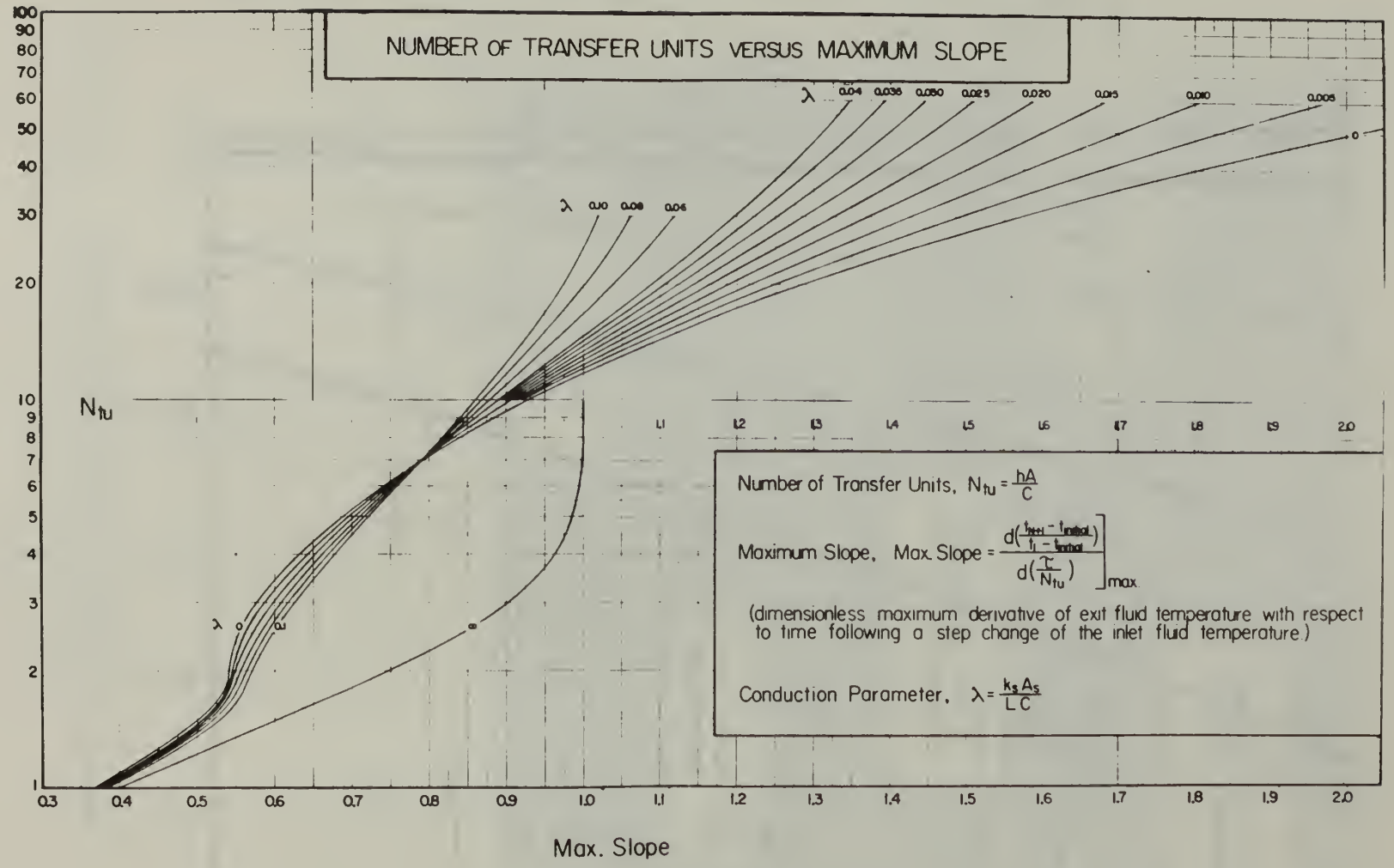


Figure 14. N_{tu} Versus Maximum Slope With Conduction Parameter (Max. Slope, .3-2.05)

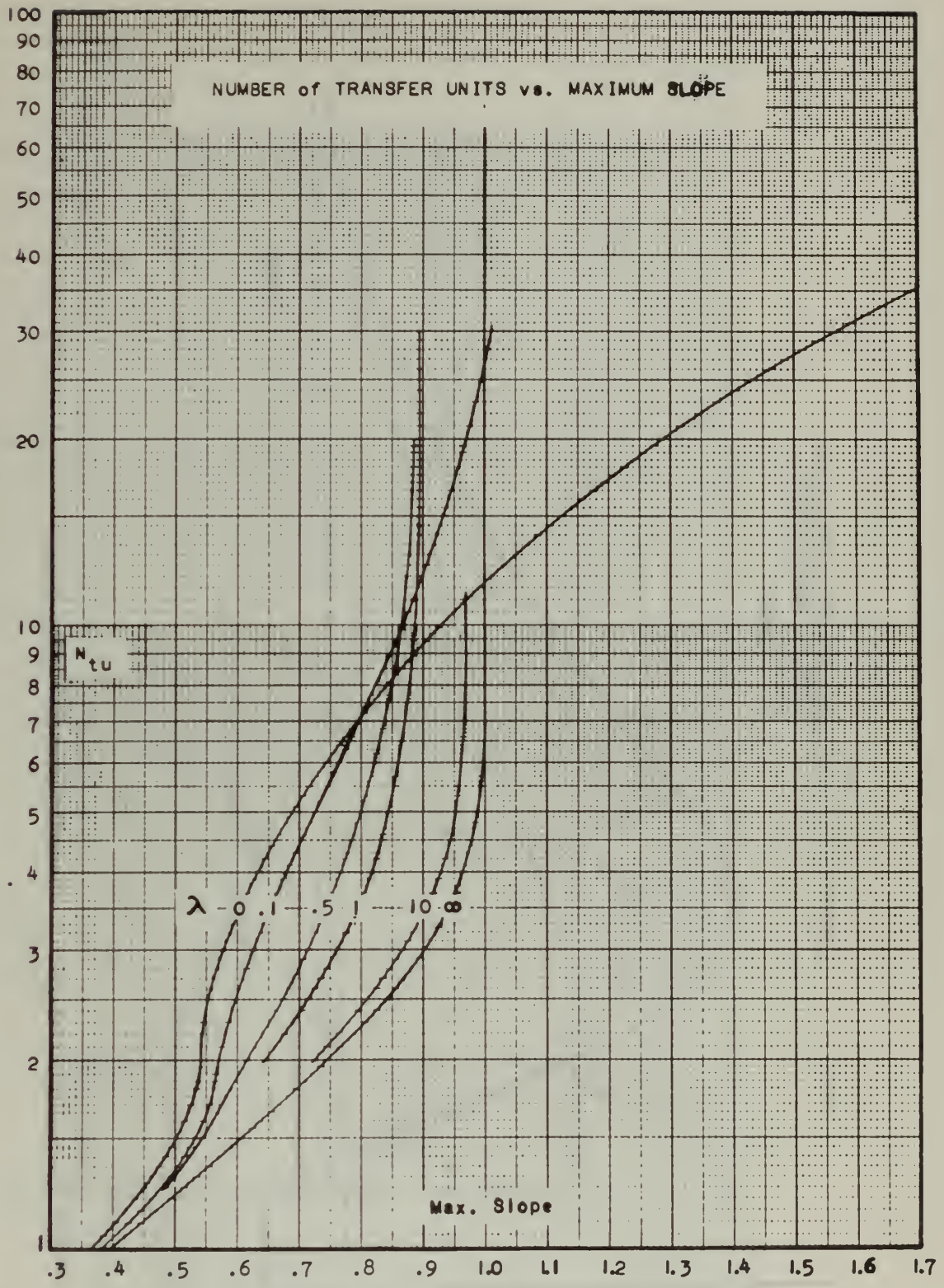


Figure 15. N_{tu} Versus Maximum Slope With Conduction Parameter (Max. Slope .3-1.7)

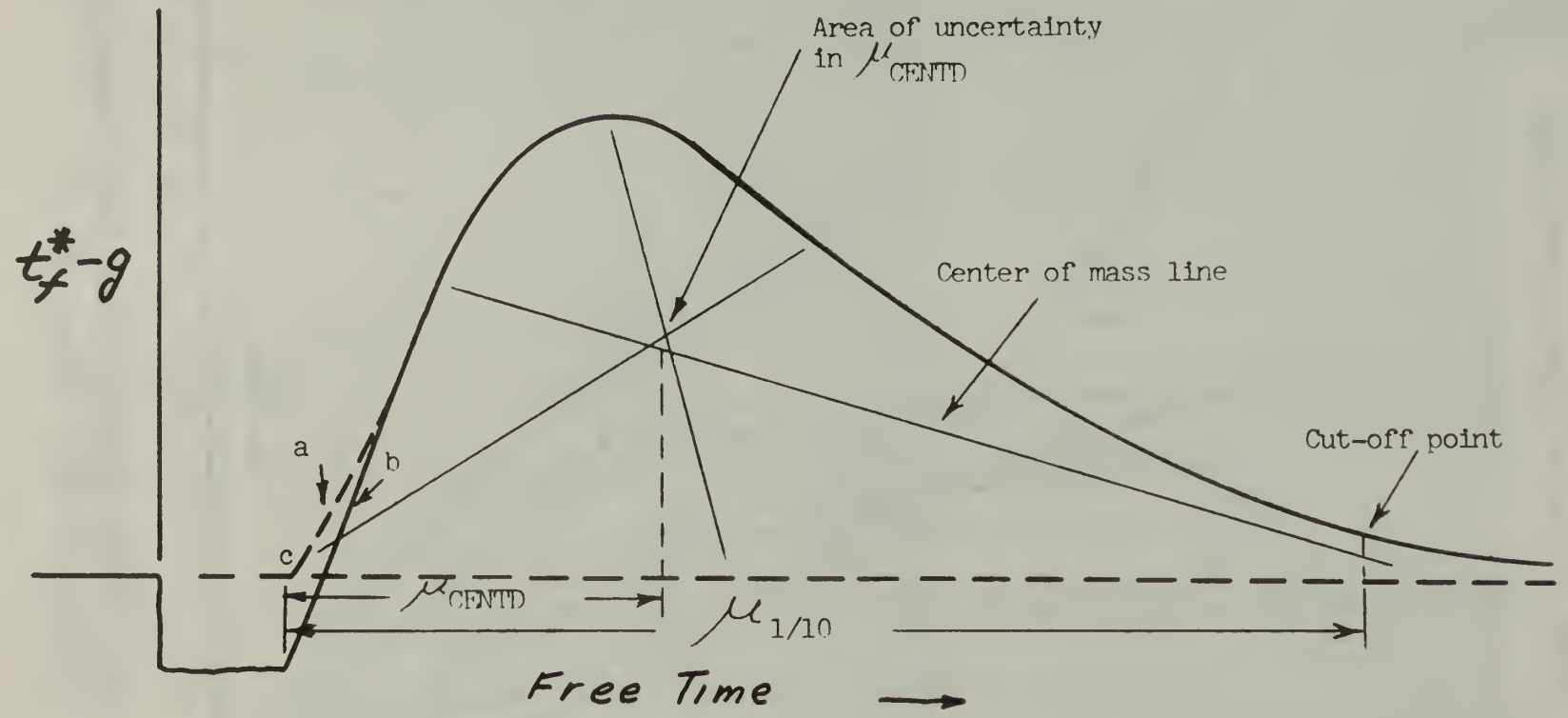


Figure 16. Finding μ_{CENTD} From Temperature-Time Trace

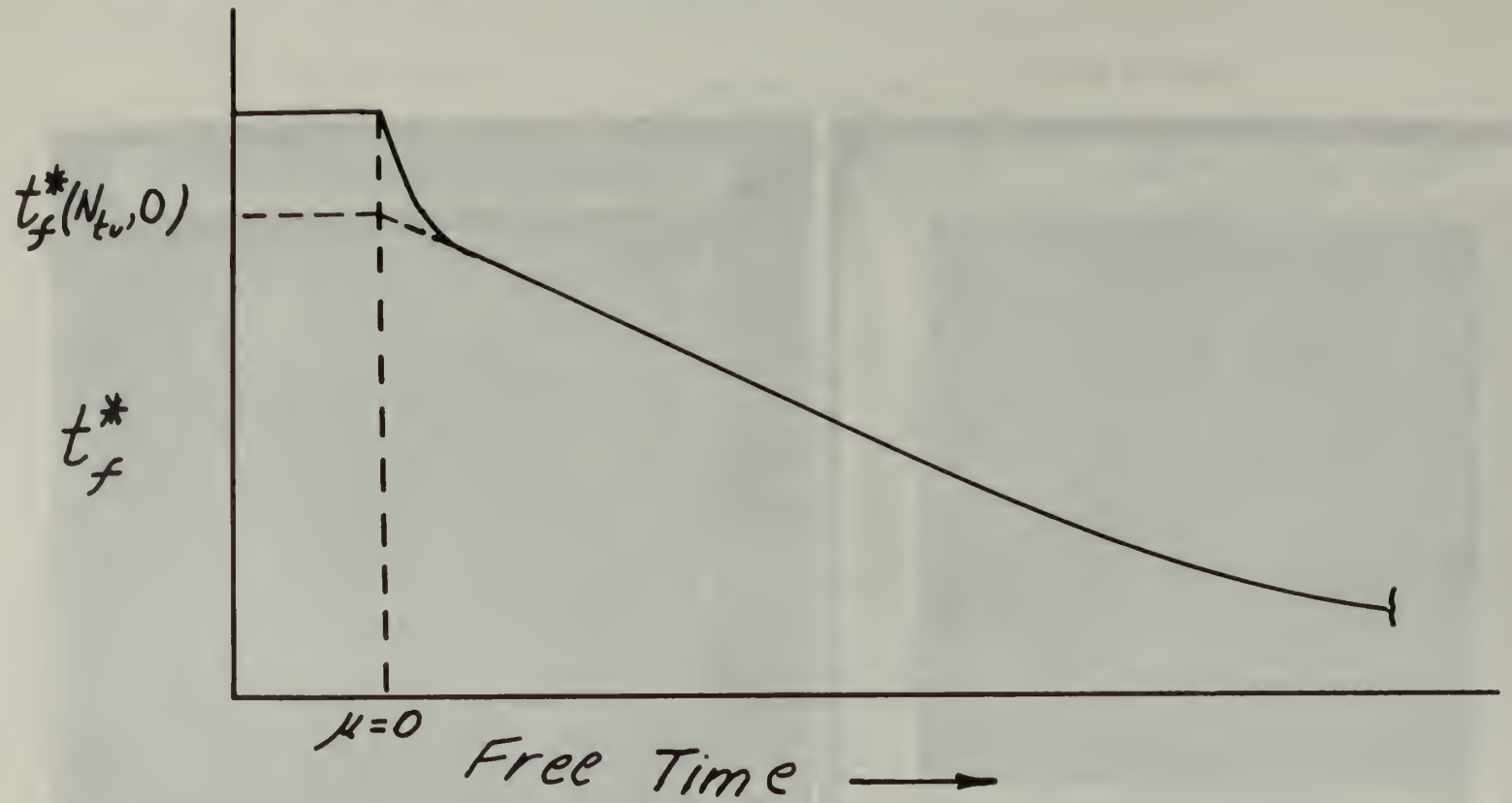
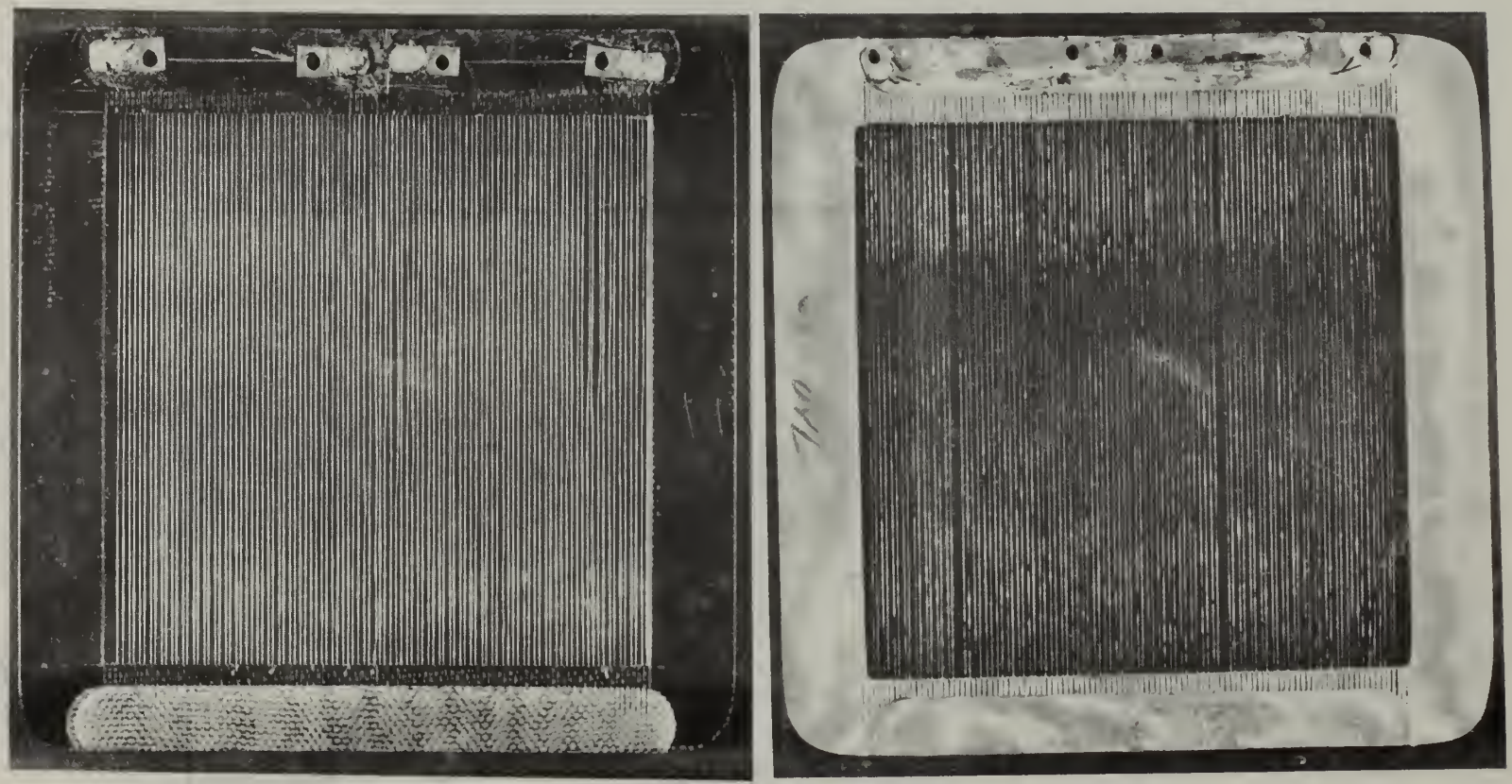


Figure 17. Finding t_f^* From Temperature-Time Trace



.003 in. Wire

.001 in. Wire

Figure 18. Photo of .003 in. Wire and .001 in. Wire Heater Frames

CERCOR T20-38

	FRICTION DATA		HEAT TRANSFER DATA						
RUN	NR	F	COND PARAM	MAX SLOPE	NTU	NR	J	ALFA	MDOT
1	121.94	0.12256	0.00016	0.96899	10.99	120.20	0.02193	0.1034	143.99
2	121.94	0.12256	0.00016	0.96069	10.78	120.20	0.02151	0.1034	143.99
3	170.82	0.09094	0.00011	0.82309	7.65	168.38	0.01526	0.1518	201.71
4	170.82	0.09094	0.00011	0.83786	7.96	168.38	0.01538	0.1518	201.71
5	218.00	0.07317	0.00009	0.74032	5.99	214.88	0.01195	0.1936	257.25
6	218.00	0.07317	0.00009	0.74693	6.11	214.88	0.01220	0.1936	257.25
7	283.11	0.05811	0.00007	0.66179	4.53	279.06	0.00904	0.2517	334.41
8	291.10	0.05577	0.00007	0.67145	4.70	286.94	0.00938	0.2587	343.74
9	291.10	0.05577	0.00007	0.66321	4.56	286.94	0.00909	0.2587	343.74
10	373.39	0.04514	0.00005	0.60957	3.61	368.05	0.00720	0.3320	441.09
11	373.39	0.04514	0.00005	0.60227	3.48	368.05	0.00694	0.3320	441.06
12	410.75	0.04193	0.00005	0.59208	3.29	404.88	0.00657	0.3653	485.31
13	413.68	0.04156	0.00005	0.54424	2.21	407.76	0.00442	0.3675	488.33
14	413.68	0.04156	0.00005	0.54417	2.21	407.76	0.00441	0.3675	488.33
15	507.81	0.03558	0.00004	0.52206	1.62	500.55	0.00324	0.4517	600.11
16	507.81	0.03558	0.00004	0.52299	1.63	500.55	0.00325	0.4517	600.11
17	634.23	0.02991	0.00003	0.46833	1.33	625.16	0.00266	0.5640	749.40
18	634.23	0.02991	0.00003	0.47215	1.35	625.16	0.00269	0.5640	749.40
19	779.90	0.02547	0.00002	0.46979	1.34	768.75	0.00267	0.6935	921.46
20	779.90	0.02547	0.00002	0.47470	1.36	768.75	0.00272	0.6935	921.46

Table I

SOLAR 4, TRIANGULAR FIN SOLID 430 STAINLESS 5 MIL

	FRICTION DATA		HEAT TRANSFER DATA						
RUN	NR	F	COND PARAM	MAX SLOPE	NTU	NR	J	ALFA	MDOT
1	54.42	0.21485	0.07671	0.99009	18.15	53.63	0.05548	0.0146	35.00
2	54.47	0.21463	0.07666	0.99099	18.22	53.69	0.05572	0.0146	35.03
3	59.94	0.19986	0.06965	0.97489	15.91	59.08	0.04864	0.0161	38.55
4	74.82	0.15910	0.05580	0.94810	13.16	73.74	0.04023	0.0201	48.12
5	74.92	0.16191	0.05572	0.94662	13.07	73.84	0.03996	0.0201	48.19
6	88.56	0.13338	0.04715	0.90363	10.68	87.29	0.03265	0.0238	56.94
7	138.23	0.09011	0.03018	0.78149	6.77	136.24	0.02070	0.0371	88.96
8	158.11	0.07972	0.02638	0.75066	6.08	155.84	0.01857	0.0425	101.76
9	361.06	0.03836	0.01156	0.51902	1.60	355.87	0.00488	0.0969	232.23
10	361.06	0.03767	0.01156	0.50982	1.53	355.87	0.00468	0.0969	232.23
11	388.66	0.03710	0.01068	0.51669	1.58	383.10	0.00483	0.1049	251.44
12	388.66	0.03710	0.01068	0.51548	1.57	383.10	0.00481	0.1049	251.44
13	504.96	0.02864	0.00828	0.46115	1.29	497.69	0.00394	0.1353	324.26
14	530.58	0.02837	0.00782	0.46356	1.30	522.99	0.00397	0.1433	343.26
15	530.58	0.02837	0.00782	0.46007	1.29	522.99	0.00393	0.1433	343.26
16	530.58	0.02837	0.00782	0.46286	1.30	522.99	0.00397	0.1433	343.26
17	548.38	0.02488	0.00762	0.44526	1.23	540.48	0.00376	0.1470	352.13
18	550.92	0.02623	0.00760	0.43909	1.21	542.98	0.00370	0.1475	353.45
19	689.01	0.02236	0.00602	0.40905	1.11	679.16	0.00341	0.1860	445.76
20	689.01	0.02236	0.00602	0.41657	1.14	679.16	0.00348	0.1860	445.76

Table II

N_{tu} \ λ	0	.005	.010	.015	.020	.025	.030	.035	.040	.060	.080	.100	.500	1.0	10	∞
1.0	.368	-	-	-	.374	-	-	-	.377	.380	.382	.384	-	-	-	.400
1.1	.403	-	-	-	.408	-	-	-	.413	.417	.420	.425	-	-	-	.445
1.2	.434	-	-	-	.440	-	-	-	.445	.447	.452	.459	-	-	-	.468
1.3	.461	-	-	-	.467	-	-	-	.472	.475	.480	.487	.497	-	-	.529
1.4	.483	-	-	-	.489	-	-	-	.494	.498	.503	.511	.522	-	-	.568
1.5	.502	-	-	-	.507	-	-	-	.512	.517	.521	.530	.542	-	-	.603
1.6	.517	-	-	-	.522	-	-	-	.527	.530	.536	.544	.560	-	-	.637
1.8	.536	-	-	-	.539	-	-	-	.542	.547	.553	.561	.569	-	-	.697
2.0	.541	-	-	-	.545	-	-	-	.545	.556	.563	.571	.615	.646	.723	.748
2.2	.544	-	-	-	.549	-	-	-	.551	.566	.574	.582	.640	.677	.764	.791
2.4	.545	-	-	-	.557	-	-	-	.567	.577	.585	.592	.662	.703	.795	.827
2.6	.557	-	-	-	.566	-	-	-	.577	.587	.595	.603	.682	.726	.824	.857
2.8	.567	-	-	-	.577	-	-	-	.587	.596	.606	.615	.699	.745	.850	.882
3.0	.577	-	-	-	.587	-	-	-	.598	.606	.617	.626	.714	.761	.869	.903
3.2	.587	-	-	-	.596	-	-	-	.609	.619	.628	.637	.727	.775	.886	.920
3.4	.596	-	-	-	.610	-	-	-	.620	.630	.640	.647	.735	.787	.899	.934
3.6	.604	-	-	-	.621	-	-	-	.631	.641	.650	.658	.744	.796	.911	.946
3.8	.621	-	-	-	.632	-	-	-	.642	.652	.660	.668	.756	.807	.920	.956
4.0	.632	-	-	-	.643	-	-	-	.653	.662	.670	.678	.767	.815	.928	.964
4.5	.660	-	-	-	.670	-	-	-	.678	.687	.694	.701	.784	.831	.941	.978
5.0	.688	-	-	-	.697	-	-	-	.704	.711	.717	.722	.800	.843	.951	.987
5.5	.715	-	-	-	.722	-	-	-	.727	.733	.737	.742	.812	.852	.956	.992
6.0	.741	-	-	-	.746	-	-	-	.750	.753	.757	.760	.822	.859	.960	.995
6.5	.767	-	-	-	.769	-	-	-	.771	.773	.774	.776	.830	.865	.962	-
7.0	.792	-	-	-	.792	-	-	-	.791	.791	.791	.792	.837	.870	.964	1.000
7.5	.816	-	-	-	.812	-	-	-	.810	.808	.806	.805	.844	.874	.965	-
8.0	.840	-	-	-	.832	-	-	-	.827	.824	.821	.817	.849	.877	.966	-
9.0	.885	-	-	-	.872	-	-	-	.861	.853	.847	.840	.858	.882	.967	-
10.0	.929	.922	-	.911	.906	.901	.897	.893	.890	.880	.869	.860	.864	.886	.968	1.000
11.0	.970	.956	.953	.946	.939	.933	.927	.921	.917	.901	.888	.878	.870	.889	.968	-
12.0	1.010	.994	.988	.979	.970	.962	.955	.948	.942	.922	.906	.893	.873	-	-	-
13.0	1.049	1.034	1.022	1.009	.999	.990	.980	.973	.965	.941	.922	.907	.875	-	-	-
14.0	1.085	1.068	1.053	1.039	1.027	1.016	1.005	.996	.987	.958	.937	.921	.877	-	-	-
15.0	1.121	1.102	1.085	1.068	1.053	1.040	1.028	1.017	1.007	.975	.950	.932	.879	.893	-	-
16.0	1.156	1.133	1.112	1.094	1.077	1.063	1.049	1.037	1.026	.990	.963	.942	.881	-	-	-
18.0	1.223	1.193	1.167	1.144	1.123	1.105	1.088	1.073	1.060	1.016	.984	.960	.885	.895	-	-
20.0	1.286	1.249	1.217	1.189	1.164	1.143	1.123	1.105	1.089	1.039	1.003	.975	.887	.894	-	1.000
22.0	1.347	1.302	1.264	1.231	1.202	1.177	1.154	1.134	1.116	1.059	1.018	.987	.889	-	-	-
24.0	1.404	1.352	1.308	1.269	1.237	1.208	1.182	1.160	1.140	1.077	1.032	.997	.891	-	-	-
26.0	1.460	1.399	1.348	1.305	1.268	1.236	1.208	1.183	1.161	1.092	1.043	1.005	.893	-	-	-
28.0	1.515	1.444	1.387	1.339	1.298	1.262	1.231	1.204	1.180	1.106	1.053	1.013	.894	-	-	-
30.0	1.565	1.487	1.423	1.370	1.325	1.286	1.253	1.224	1.198	1.118	1.061	1.019	.895	-	-	1.000
32.0	1.617	1.528	1.458	1.399	1.351	1.309	1.273	1.241	1.214	-	-	-	-	-	-	-
34.0	1.665	1.568	1.490	1.427	1.374	1.330	1.291	1.258	1.228	-	-	-	-	-	-	-
36.0	1.712	1.605	1.521	1.453	1.397	1.349	1.308	1.273	1.242	-	-	-	-	-	-	-
38.0	1.757	1.641	1.551	1.478	1.418	1.367	1.324	1.287	1.254	-	-	-	-	-	-	-
40.0	1.801	1.676	1.579	1.501	1.437	1.384	1.339	1.300	1.266	-	-	-	-	-	-	1.000
45.0	1.908	1.757	1.643	1.554	1.481	1.422	1.372	1.328	1.292	-	-	-	-	-	-	-
50.0	2.010	1.833	1.702	1.601	1.520	1.455	1.400	1.353	1.313	-	-	-	-	-	-	1.000
55.0	2.107	1.902	1.756	1.644	1.555	1.483	1.425	1.375	1.332	-	-	-	-	-	-	-
60.0	2.199	1.967	1.803	1.683	1.585	1.508	1.445	1.392	1.347	-	-	-	-	-	-	1.000

Maximum Slope

Table III N_{tu} as a Function of Maximum Slope and Longitudinal Conduction Parameter

INITIAL DISTRIBUTION LIST

		No. Copies
1.	Defense Documentation Center Cameron Station Alexandria, Virginia 22314	20
2.	Library Naval Postgraduate School Monterey, California 93940	2
3.	Department of Mechanical Engineering Naval Postgraduate School Monterey, California 93940	2
4.	Naval Ship Systems Command (Code 2052) Navy Department Washington, D. C. 20360	1
5.	Professor P. F. Pucci Department of Mechanical Engineering Naval Postgraduate School Monterey, California 93940	4
6.	LT Marco J. Bruno, USN USS RANGER (CVA-61) % FPO San Francisco, Calif. 96650	2

Unclassified
Security Classification

DOCUMENT CONTROL DATA - R & D

Security classification of title, body of abstract and indexing annotation must be entered when the overall report is classified)

ORIGINATING ACTIVITY (Corporate author)
Naval Postgraduate School
Monterey, California 93940

2a. REPORT SECURITY CLASSIFICATION
Unclassified

2b. GROUP
NA

REPORT TITLE
Experimental Techniques to Determine N_{tu} of Compact Heat Exchanger Surfaces

DESCRIPTIVE NOTES (Type of report and inclusive dates)
None

AUTHOR(S) (First name, middle initial, last name)
Marco Joseph Bruno

REPORT DATE	7a. TOTAL NO. OF PAGES	7b. NO. OF REFS
September 1968	77	18

8a. CONTRACT OR GRANT NO	9a. ORIGINATOR'S REPORT NUMBER(S)
NA	NA
b. PROJECT NO	
c.	9b. OTHER REPORT NO(S) (Any other numbers that may be assigned this report)
d.	NA

DISTRIBUTION STATEMENT
[redacted]

11 SUPPLEMENTARY NOTES	12 SPONSORING MILITARY ACTIVITY
None	Naval Postgraduate School Monterey, California 93940

ABSTRACT

Two new transient testing techniques were evaluated; the centroid method developed by Kohlmayr and the time zero intercept technique. The zero intercept method was found to be the most promising of the two but is limited to values of $N_{tu} \leq 2.5$. The centroid technique can be used effectively when the value of N_{tu} is less than 5.0.

A heater system made of .001 inch diameter nichrome wire was designed and tested to determine its effect on the transient testing of matrix type heat exchangers. Because the design showed no improvement in the test results and was unreliable its use was discontinued.

DD FORM 1 NOV 65 1473 (PAGE 1)
S/N 0101-807-6811

Unclassified.
Security Classification

A-31408

14 KEY WORDS	LINK A		LINK B		LINK C	
	ROLE	WT	ROLE	WT	ROLE	W
Heat Exchangers						
Heat Transfer Surface						
Regenerators						
Recuperators						

thesB8264
Experimental techniques to determine N/t
DUDLEY KNOX LIBRARY
3 2768 00417117 3
DUDLEY KNOX LIBRARY